



Review

# Gas Emissions from Lithium-Ion Batteries: A Review of Experimental Results and Methodologies

Elna J. K. Nilsson <sup>1,\*</sup> and Annika Ahlberg Tidblad <sup>2,3</sup><sup>1</sup> Combustion Physics, Department of Physics, Lund University, P.O. Box 118, SE 221 00 Lund, Sweden<sup>2</sup> Volvo Car Corporation, SE 405 31 Gothenburg, Sweden; annika.ahlberg.tidblad@volvocars.com<sup>3</sup> The Ångström Advanced Battery Center, Department of Chemistry–Ångström, Uppsala University, P.O. Box 538, SE 751 21 Uppsala, Sweden

\* Correspondence: elna.heimdal\_nilsson@fysik.lu.se

**Abstract:** Gas emissions from lithium-ion batteries (LIBs) have been analysed in a large number of experimental studies over the last decade, including investigations of their dependence on the state of charge, cathode chemistry, cell capacity, and many more factors. Unfortunately, the reported data are inconsistent between studies, which can be explained by weaknesses in experimental methodologies, the misinterpretation of data, or simply due to the comparison of datasets that build on different prerequisites. In the present work, the literature on gassing from battery components and battery cells is reported, with a focus on vent gas composition resulting from internal chemical processing in the battery and excluding studies where the gases are combusted after venting. The aim is to identify datasets of high quality that contribute to the advancement of our understanding of gas emissions from LIBs. Gas compositions from different stages in the gassing process are included, starting with the slow formation of gases during normal operation via mild thermal events to a thermal runaway (TR) with extensive gas production. Available published data are used to map gas quantity and composition from LIBs undergoing venting, with or without a TR, and to identify gaps in understanding and the need for further research.



**Citation:** Nilsson, E.J.K.; Ahlberg Tidblad, A. Gas Emissions from Lithium-Ion Batteries: A Review of Experimental Results and Methodologies. *Batteries* **2024**, *10*, 443. <https://doi.org/10.3390/batteries10120443>

Academic Editors: Jun Xu and Xiang Gao

Received: 1 November 2024

Revised: 6 December 2024

Accepted: 10 December 2024

Published: 14 December 2024



**Copyright:** © 2024 by the authors. Licensee MDPI, Basel, Switzerland. This article is an open access article distributed under the terms and conditions of the Creative Commons Attribution (CC BY) license (<https://creativecommons.org/licenses/by/4.0/>).

## 1. Introduction

### 1.1. The Research Field

Research on safety related to lithium-ion batteries (LIBs) has rapidly increased over the last couple of decades, motivated by the continually expanding use of this battery type in electric vehicles (EVs) and a variety of electrical devices. An important aspect of LIB safety is the potential for the formation of flammable and toxic gases, which occur to a small extent during regular use but can accelerate as a result of internal LIB cell failure or external interference. To understand and mitigate unwanted gas formation, research on LIB failure has been expanding, spanning a wide range of studies from mechanistic studies on the degradation of cell materials to full-scale fire studies on EVs. An overview of the research field is given in Figure 1, where the main levels of the physical system under investigation are given in the horizontal direction: LIB cell components, followed by the cell level, and finally, the assembled battery. From the ordinate line, the degree of severity of conditions is clearly increasing, which can essentially be connected to temperature regimes: normal operation is around ambient temperatures, moderate heating is in the range of 80–150 °C, thermal runaway is characterised by rapid self-heating starting at around 150–220 °C and increasing to about 1000 °C, and finally, fire can occur at combustion temperatures. The mechanisms resulting in gassing in these regimes are partly different and require different experimental methodologies to be fully understood.

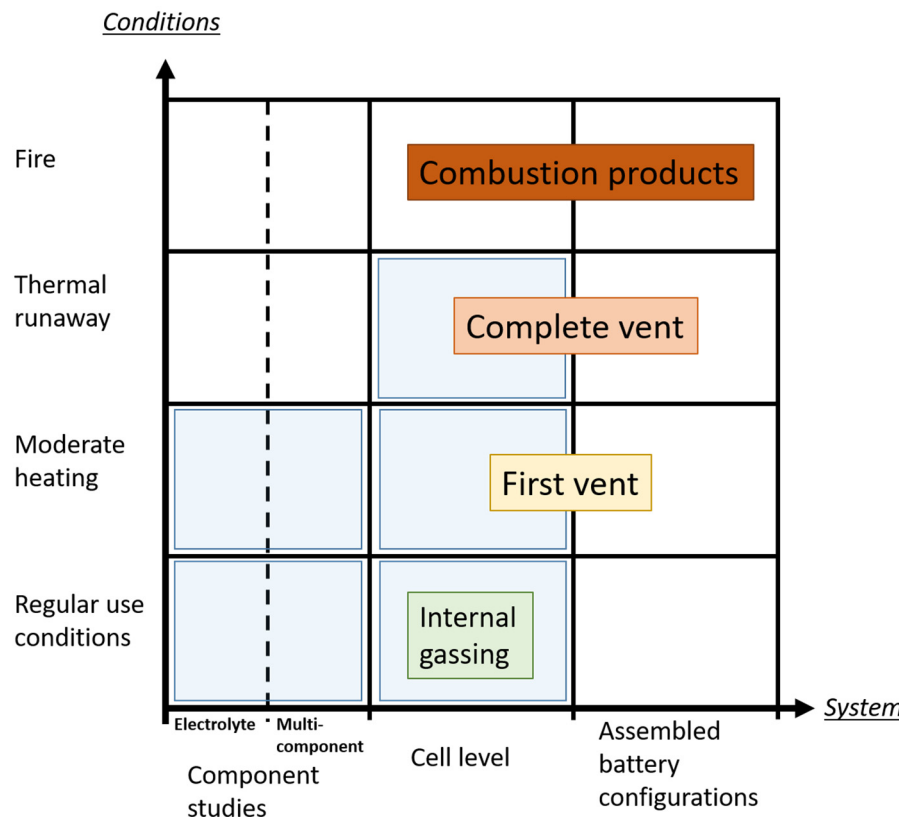


**Figure 1.** Schematic representation of the research field, where areas shaded in blue are the aspects focused on in the present review.

The literature includes studies on the composition of gases directly vented from the LIB cell before ignition and combustion occurs, as well as combustion products in case of a fire. In addition, selected components like electrolytes are studied separately to yield information on their contribution from different parts of the battery cell. The gassing process comprises different processes and phases, depending on multiple factors, such as the type of venting, temperature, cell chemistry (referring to cathode material), state of charge (SOC), etc., which are thought to determine the degree of chemical processing and the hazardousness of the vented gases in terms of flammability and toxicity.

The evolving research on LIB failure can be exemplified by a recent bibliometric analysis by Wang et al. [1], where keywords such as “battery” and “thermal hazard/risk/danger” were used to identify 707 publications in peer-review journals since 2010, with the majority produced since 2020. Keyword analysis in that work indicates an increasing tendency to use words like “fire” and “failure”. Keywords that were hardly used in the first part of the studied period but that emerged in the second half are “combustion”, “heat release rate”, and “fire hazard”, indicating an increased focus on these aspects. This is indicative of an increased focus on fire safety issues and the call for an improved fundamental understanding of fire and safety hazards related to LIBs.

Over the last decade, numerous review papers have been published, targeting various aspects of battery safety, such as heat release and gas formation and the mitigation of battery fires. An early review published already in 2012 by Wang et al. [2] was highly cited, but authors from the same group published a more extensive review in 2019 [3]. The later publication is the most extensive description available of the chemical mechanisms occurring inside the battery during abuse test conditions that are used to assess the safety performance of LIBs. That work also includes an overview of experimental studies of gases from abused LIBs, but it is not exhaustive on that point. An overview of gassing studies up until 2017 was presented as part of the experimental work by Fernandes et al. [4], and more recently, Qiu et al. [5] reviewed the research progress on LIB vent gas studies,

with a particular focus on the effects of ageing on gas production from thermal failure. Heat release from LIBs has been reviewed by Ghiji et al. [6], including both experimental and numerical studies to understand parametric factors on fire risk and heat release. The recent meta-analysis by Rappsilber et al. [7] points to the unfortunate fact that experimental studies by different research groups do not give a consistent picture of heat release and gassing from LIB. The discrepancies are thought to originate from the use of various experimental designs, analysis tools and procedures. Furthermore, although abuse studies give valuable information about how the battery may react in abnormal abuse conditions, their correlation to spontaneous fire incidents caused by the battery's internal failure is not straightforward. Thermal runaway (TR) caused by an internal short circuit fault in a cell, which may or may not propagate within the battery, is not necessarily a result of abuse. Hence, thermal runaway and thermal propagation failures have been notoriously challenging to replicate and study experimentally; a forced cell TR in a laboratory context evolves differently from a spontaneous TR in an LIB cell in a real application.

A review on off-gas composition and volume was recently published by Bugryniec et al. [8], with a particular focus on toxic compounds and total gas volumes. They included 60 published studies and outlined trends in gassing related to SOC, cell chemistry, and cell geometry (cylindrical, pouch, prismatic). A clear trend found was that the gas volume scaled linearly with cell capacity, but apart from that, there were significant variations in the results. One drawback in the meta-analysis was that experimental studies at various conditions were compared; for example, datasets both with and without combustion were included, which may explain a significant part of the inconsistencies.

As interpreted by the authors of the present work, experimental results are sometimes misinterpreted due to a lack of background information. Also, comparisons of different studies are made based on the assumption that they are targeting the same property or process. As an example, CO<sub>2</sub> concentrations from two studies of similar LIB cells can be different if one study measured the vented gas in an inert environment, while in the other study, the gases were ignited, and the products after combustion were quantified. In the present review, published research related to gassing from LIB cells is scrutinised, and we try to evaluate the understanding gained while identifying inconsistencies in test methodologies as well as pointing out weaknesses in the reviewed studies and recommending further research to strengthen scientific knowledge.

## 1.2. Brief Overview on LIB and Gassing

An LIB consists of solid and liquid material that is ideally stable over time but instead undergoes a continuous but slow degradation process referred to as "ageing" [9–11]. During ageing, the battery constituents undergo unwanted decomposition and chemical reactions, forming modest amounts of gas phase compounds that may eventually make the battery cell become pressurised and contribute to the irreversible swelling of the cell. Chemical reactions and decomposition are quite often temperature-dependent [11], which is the reason why batteries age faster in a warmer environment. The composition of gases in an aged battery has not been investigated to any significant extent, and it appears to often be assumed that the composition and hazardous properties of gas resulting from the ageing process are the same, or similar, to those occurring due to thermal, mechanical, and electrical abuse. This may explain the lack of published studies on LIB gassing due to ageing. Gas composition from aged LIB cells under abuse conditions has been shown to be different from that of fresh cells, which indicates that there may be some "chemical pre-processing" in an LIB cell during normal operation. This calls for further work on gas formation in LIB cells during ageing. The current state of knowledge on gas composition due to ageing is reviewed in Section 2 of the present work.

When a battery is exposed to abuse (thermal, electrical, or mechanical, as outlined by Ghiji et al. [6]), the rate of the internal chemical processing accelerates as a result of one or several factors: increased temperature; the positive and negative battery electrodes are in direct contact with each other and with the electrolyte; or the electrode is in direct

contact with external reactive materials like oxygen and humidity in the air. The resulting chemical reactions are exothermic and produce heat that further increases the temperature of the system and accelerates the chemical processing and breakdown of materials. In this work, we call the self-heating process of the battery a “thermal event”. Depending on the balance between heat production and the efficiency of heat dissipation to the surroundings, the thermal event may stop and self-quench as the battery cools down. However, if the generated heat cannot be dissipated at a sufficient rate, it may result in a “thermal runaway” (TR), which is a more severe thermal event where an uncontrolled sequence of exothermic chemical reactions results in rapid temperature increase and extensive gas production [3]. TR results in the extensive venting of the battery, potentially in an uncontrolled manner, and the ejected gases may ignite and cause a fire. In addition to gases, a venting battery will also expel solid material and fine particulate matter [12,13], which has implications for the health and overall risk assessment of LIB venting and fires.

The processes involved in a thermal event in an LIB have been explained comprehensively by, among others, Wang et al. [3] and Qiu et al. [5] and are just briefly outlined here. As the battery cell is overheated, the first step towards TR is commonly the breakdown of the SEI layer on the graphite anode, which occurs at about 90–120 °C. At these temperatures, volatile electrolyte components such as dimethyl carbonate (DMC) can start to evaporate and decompose. The SEI protects the graphite from direct contact with the electrolyte and is formed on the anode surface during cell formation. In the process, there is a release of stable lithium (Li) compounds, small hydrocarbons like ethylene ( $C_2H_4$ ), carbon dioxide ( $CO_2$ ) and oxygen molecules ( $O_2$ ). As the SEI breaks down, the anode material can react with the electrolyte, and the electrolyte can also react with Li to form lithium carbonate ( $LiCO_3$ ) and  $C_2$ – $C_3$  hydrocarbons. When the separator melts at temperatures in the range of 135–165 °C, the electrical contact between the anode and cathode can result in an ISC and, thereby, self-discharge. As the temperature increases further in the range of 150–310 °C, the cathode begins to decompose and release oxygen. As the temperature reaches 200 °C and higher, all components of the electrolyte start to decompose exothermically, upon which  $CO_2$ , hydrogen fluoride (HF), hydrocarbons, and various fluorinated hydrocarbon gases are formed. Oxygen released from the cathode material can react with the solvent or other hydrocarbon components, driving the production of final oxidation products  $CO_2$  and  $H_2O$ , but also the intermediate hydrocarbons, CO and  $H_2$ , depending on the availability of  $O_2$ . For further details, we refer to the review by Wang et al. [3] and the references therein.

Gaseous species formed in LIB cells include  $CO_2$ , CO,  $O_2$ ,  $H_2$ ,  $CH_4$ ,  $C_2H_4$ , and  $C_2H_6$ , higher hydrocarbons, including the carbonates in the electrolyte, and fluorinated compounds like HF and fluoromethane ( $CH_3F$ ) [3]. These compounds are found in gases from aged batteries, from batteries that vented after a minor thermal event, but also from severe venting during a TR. The relative amount of these compounds varies notably depending on the degree of chemical processing, which is attributed to the effects of a range of parameters, such as SOC at the time of gas formation and venting, battery chemistry, age, battery geometry, and potentially a range of other factors. The composition of the gas mixture, as well as the total amount of gases being vented from a battery during TR, will affect the flammability and toxicity and, thus, the severity of a potential incident. To increase understanding of these factors, LIB cells have, to a large extent, been studied in different experimental configurations where a thermal event is triggered, and the gases and heat release are determined. An overview of the experimental methods is given in Section 3 of the present work. In addition to the research on complete LIB cells, studies have also been conducted on battery components, one by one and in combination. These studies provide a fundamental understanding of the processes occurring in an LIB, as explained in Section 4.

### 1.3. Scope of the Present Review

Experimental studies of gassing from LIBs can be divided into two categories: vent gas studies and combustion product studies. In vent gas studies, the composition of the gas mixture escaping the chemical system is investigated, while in combustion product

studies, gases are sampled during or after a fire. From the aspect of the fundamental understanding of the TR and the chemical processing in the battery, vent gas studies are of high importance since they reveal the types and amounts of gases being produced in the LIB. Hazard assessments require information about gas composition, gas volume, and, ideally, also initial conditions with respect to gas temperature, characterising a gas vent from an LIB. Using this information, the severity of an incident, for example, whether a fire is likely to start, can be evaluated. The interpretation of the mentioned data typically also requires background information about the LIB: cathode chemistry, electrolyte composition, SOC, cell geometry (pouch, prismatic, cylinder), cell capacity as well as, in the case of a battery pack, the cell configuration and connections inside the battery.

Experimental work often provides information on the vent gas composition target at one or several of the following levels:

1. Solvent studies address the properties of relevant carbonates, including their evaporation and decomposition characteristics. The value of these studies is understanding the stability of the different carbonates and their decomposition products. It is, however, important to note that properties like decomposition temperature may be altered depending on the chemical environment, and the results from solvent studies cannot be fully extrapolated to LIB conditions.
2. Electrolyte studies of mixtures of carbonate and lithium salt are needed to understand how the presence of salt affects the evaporation and decomposition of the electrolyte, which is important in the early steps of a thermal event.
3. The electrode material, in combination with the electrolyte in a half-cell, is studied to gain an understanding of the chemical interactions between these materials.
4. The composition of gases in a cell during regular use conditions provides information about the chemical environment at the onset of a thermal event, which is particularly important for aged cells.
5. The total volume of gas from LIB cells subject to internal failure caused by abuse conditions is important for an assessment of fire and explosion risks.
6. The composition of gas vented from LIB cells subject to internal failure caused by abuse conditions provides information that allows the assessment of flammability and toxicity.
7. Thermal evolution in LIB cells subject to failure caused by abuse conditions, including information about onset temperature for TR, is important to assess the risk of spread of TR in a battery pack.
8. Studies on several cells or a full pack are necessary to understand how findings from single-cell studies can be extrapolated to larger systems.
9. The composition of combustion gases from LIB fires provides information that enables risk assessment.

Unfortunately, it is practically impossible to study spontaneous internal failures not triggered by abuse in experimental settings since the occurrence of these events is very rare. A forced TR using different types of abuse triggers is currently the only available path, and it has been demonstrated that the choice of the TR method influences the cell response [14], depending on the accelerating effect of the chosen method as well as the difference in the localised vs. general activation of the TR reactions inside the cell.

In the present work, the main focus is on gas composition in vented gases from LIB cells, point 6 in the list above, but also the literature on points 2–4 is reviewed since they can provide supporting data in understanding the events.

Studies of assembled battery configurations at the pack level and complete devices such as electric vehicles (EVs) are dominated by combustion studies. While measurements of gases from evolved battery fires have been extensively reported in the literature, they are found to be of less importance for understanding the onset and different stages of an event and knowledge with the potential to mitigate or prevent future events. The correlation between the reaction mechanism and the related reaction products created by the test methods and the safety events and associated cell responses under real conditions

in the field are largely missing. To be able to assess the relevance of the experimental test results compared to different types of field responses to safety events, it is also critical to understand the level of abuse, e.g., how much external energy was added to the component/cell/battery assembly to produce the observed thermal event, since this is a measure of the experimental acceleration factor used. Experimental instrumentation can also be an accelerator if it results in uncharacteristic modifications of the test object; for example, it introduces alternative vent paths or oxygen ingress into the battery, enabling more intense fire events than would have been possible in the original battery design.

The motivation behind other published reviews on LIB vent gas research is commonly one of the following: (1) to understand the underlying mechanisms and ascertain their dependence on various parameters (SOC, energy density, age, etc.); (2) the quantification of factors related to heat release and gas release; and (3) the investigation of prevention and mitigation strategies. Ideally, the research data and conclusions should provide information that enables the development of successful safety strategies and the design of safe LIBs. To achieve these goals, the research needs to be designed in such a way that the produced data are not a mere investigation of a particular battery but that the results can be extrapolated to other conditions or, together with other datasets, provide valuable generalised information. The value of some studies is, unfortunately, hampered by a limited scope. In the review presented here, one important aim is to identify datasets of value for the overall understanding and quantification of vent gases from LIBs.

The present review summarises the current understanding of gas composition from different stages in the gassing process from LIBs, starting at ageing and the slow formation of gases, via mild thermal events to TR with extensive gas production. The published data are used to map gas quantity and composition from LIBs undergoing venting, with or without a TR, and to identify gaps in understanding and the need for further research.

The main discussion in this review is on major constituent gases (>1% of total gas volume) that contribute to the fire and explosion risks. CO, H<sub>2</sub>, and hydrocarbons are the main drivers of combustion in the present context, and CO<sub>2</sub> plays an important role since it has an inerting effect. In addition, the potential presence of O<sub>2</sub> in the vented gases is discussed based on available knowledge and data. In this review, papers that make an exhaustive characterisation of minor components of importance to the toxicity of the off-gases are included, but no in-depth discussion on toxicity is provided. Hydrogen fluoride (HF) is, by some, considered an important toxic compound vented from LIBs, but it is not a player in a fire or explosion risk scenario and, therefore, has not been reviewed in an exhaustive manner. However, the experimental challenges related to the detection of HF and other fluorinated compounds are relevant for the discussion on experimental methodologies for vent gas studies and are discussed in this particular context.

## 2. Gassing During Normal Use Conditions

Gases are formed in an LIB cell already during the first cycling and the formation of the SEI layer when small amounts of CO<sub>2</sub> and hydrocarbons like C<sub>2</sub>H<sub>4</sub> or CH<sub>4</sub> have been detected [15,16]. During regular use, a small amount of gas is produced by slow material degradation, and this is part of the ageing process. The ageing of the battery cell and the formation of gases is an important topic in terms of quality and durability [17], but it is also relevant in investigations of malfunctioning batteries since, as shown by Essl et al. [9], ageing affects the gas composition of a battery cell that experiences TR failure.

Several studies have determined the pressure or volume increase caused by cycling under different conditions within the normal usage range, but data are scarce regarding the composition of the gas mixture.

Scharf et al. [16] investigated gas production during cell formation in their effort to gain insights into the formation process and its temperature dependence in the range from 10 to 40 °C. The production of C<sub>2</sub>H<sub>4</sub> is found to be important during cell formation with the build-up of the SEI layer when significant amounts of H<sub>2</sub> and CO are formed, with minor amounts (<1%) of O<sub>2</sub> and CO<sub>2</sub>. Gases produced during formation are removed in

the final steps of cell production and will, thus, not affect the future of the cell, but the same type of chemical reactions continue at a low rate during the lifetime of the cell, and the same products can be expected to be formed.

Raghibi et al. [15] used gas chromatography (GC) to investigate both the composition and quantity of gases formed during the normal cycling of NMC pouch cells with four different carbonate solvents and two Li-salts to reveal the potential connection between gas formation and the choice of electrolyte components. They stress that the amount of free gas in the cell depends both on the volume of gas formed and the degree to which this gas is dissolved in the liquid electrolyte. While most gases are formed by the decomposition of the cyclic ethylene carbonate (EC) during cell formation and the establishment of the SEI layer, it was also found that the shorter and more volatile linear dimethyl carbonate (DMC) produces more gas than ethyl methyl carbonate (EMC). The solubility of the gases is largely affected by Li-salts, with lithium bis(fluorosulfonyl)imide-(LiFSI)-containing electrolytes taking up more gas than the ones with the more common lithium hexafluorophosphate ( $\text{LiPF}_6$ ) [15].

An important finding by Raghibi et al. [15] was that the reactive gases  $\text{O}_2$  and  $\text{H}_2$  are dissolved in the electrolyte to a lesser extent than the more stable  $\text{CO}_2$  and hydrocarbons. This means that the reactive gases are, to a larger extent, available to react with additional gases formed during a thermal event and, thus, contribute to the chemical processing and potential production of flammable gases in a thermal event.

From the information outlined above, it is concluded that the electrolyte constituents play a role in creating a reactive environment with  $\text{O}_2$  available in a battery during normal use. The presence of  $\text{O}_2$  and  $\text{H}_2$  in aged cells may contribute to accelerated reactions if the battery cell is subject to abuse or other failure modes leading to a TR, and hence, different safety responses from aged compared to new batteries during testing conditions as well as in field incidents. Studies where thermal events were triggered in aged LIBs show that aged cells can have a different thermal response and different gas composition compared to fresh cells [9,18]. This calls for further studies on gas composition in cells during regular use conditions.

### 3. Methods Used in Li-Ion Battery Gassing Studies

Thermal events resulting in excess gassing from a LIB often originate from the spontaneous manifestation of internal cell faults but can also be a result of electrical, mechanical and thermal abuse, as explained in the review by Feng et al. [19]. Electrical abuse can be an external short circuit, overcharge, over-discharge or over-current. Mechanical abuse is crushing or the deformation or penetration of the battery cell with a nail or a rod. Thermal abuse can be either local with the initial heating of parts of a cell or involve the external heating of the full cell. The forced thermal runaway of a cell by applying some form of external abuse condition is currently the only feasible way to study battery thermal events. The most common method in experimental studies is the slow (0.5–2.0 °C/min) uniform heating of the LIB cell, which allows for a well-controlled experiment. However, the slow homogenous heating of the entire cell is not the most relevant TR trigger condition when attempting to replicate real-world failure modes, which are characterised by rapid localised heating at and around the area of the cell directly affected by the fault or abuse condition, followed by the heterogeneous heating of the rest of the cell and potentially of neighbouring cells in a battery in the case of a propagating thermal event.

As recently outlined in a work by Willstrand et al. [14], the test methodology chosen can affect the results since the dynamics of the cell response depend on the TR trigger. Thus, a deeper understanding of the different test methods to assess their applicability to evaluate different aspects of TR behaviour is needed. In the following subsection, first, the controlled external heating experiments are outlined since they constitute a large part of the gassing studies and are performed using a range of dedicated methods. This is followed by information about rapid trigger methods like nail penetration. Finally, the common gas analysis methods are outlined.

The aim is not to make exhaustive reviews of the methods but to provide the reader with some overview information and to become acquainted with the pros and cons of methods commonly used and reported in the literature. An understanding of experimental methods and how the choice of methods may affect the cell's TR response will aid in the evaluation of some of the experimental studies presented in later sections.

### 3.1. Controlled Heating Experiments

Uniform and controlled heating is the most common way to trigger thermal events and TR in laboratory studies. The advantages are that the experiment is well-controlled, and it is relatively easy to perform and monitor thermal events. The experimental setups can broadly be divided into three categories: calorimeters, direct-contact uniform heating and radiative heating. These methods have a moderate heating rate in common, often in the range of 0.5 to 2.0 °C/min and starting from ambient. This means that it takes hours to bring the LIB cell or material to temperatures where the onset of electrolyte evaporation and chemical breakdown occur. With these methods, the tested systems can be expected to have enough time to equilibrate and reach homogeneous temperatures until the start of rapid self-heating (90–180 °C). Common methods are listed in Table 1, and some more details are provided in the text.

**Table 1.** Methods for controlled heating experiments.

Abbrev.	Name	Advantage
DSC	Differential scanning calorimetry	Provide an understanding of thermal properties in LIB cell materials
ARC	Accelerating rate calorimetry	Allow close monitoring of the thermal event
TC	Tewarson calorimeter	Can be applied to fire studies
CC	Cone calorimeter	Can be applied to fire studies
HP	Heating plates and heating tape giving thermal contact	Can be designed to fit any size and shape of LIB cell and easily combined with various diagnostics and methodologies
	Radiative heating	-

Calorimeters are used to measure the heat released or absorbed during a chemical reaction or physical change. It works by allowing the transfer of heat from the tested system to a surrounding medium where the heat can be measured. There are various types of calorimeters, each designed for specific applications and with different levels of precision. The technique for accelerating the rate of calorimetry (ARC) has been widely applied in studies of the LIB electrolyte [20–22] as well as on LIB cells [23–27]. The ARC increases the temperature in discrete steps, waits for the thermal transient to decay and then monitors the temperature of the cell for a fixed time duration. If the cell temperature does not exceed a threshold value, the process is repeated at the next temperature increment. If the cell temperature increases at a rate equal to or above the threshold value, the ARC switches to the exothermic mode, during which it closely matches the cell temperature, thus maintaining an adiabatic state. Differential scanning calorimetry (DSC) is a thermoanalytical technique used to measure the difference in heat flow into a substance and a reference material as a function of temperature or time. DSC has been used to correlate TR events to the thermal stability of battery components and is often used in combination with ARC [20,21,23,28]. Tewarson calorimeters are commonly used for measuring the specific heat capacity of materials at high temperatures and have been applied to measure the heat release rate in fire studies of LIB material [29]. A cone calorimeter can be used to measure the heat release rate, smoke production rate, and other key parameters during the combustion of materials, and is, therefore, particularly valuable in fire research [30–32]. Cone calorimeters can be

combined with combustion test chambers to measure the heat release rate, as performed by Huang et al. [33].

Uniform and controlled heating can be performed on large battery cells with electrically heated plates, as exemplified by Willstrand et al. [14]. Liu et al. [34] used a heating plate to simulate TR, which resulted in a fire later on. Lammer et al. [35] used an electric resistance furnace to heat the LIB cell. There were feedthroughs for thermocouples, an inert gas inlet, and a gas sampling station.

### 3.2. Rapid Trigger Methods

In safety testing, TR is often a result of a rapidly triggered ISC by applying external thermal or mechanical abuse (localised heating, crushing, or penetration). These events can be studied in laboratory environments, but the time scales are much shorter than for the slow thermal methods described above, and therefore, it is challenging to obtain reliable information on the dynamics.

Mechanical trigger methods have been explained in detail by Liu et al. [36], who explored compression, deformation, and penetration abuse. A significant difference was found between a local trigger, such as nail penetration, compared to an abuse condition applied uniformly to the cell, like the thermal methods, as presented in a previous section, and the consequences will vary depending on where in the cell and how the trigger is applied.

Willstrand et al. [14] used three methods for the rapid triggering of TR: a patented heater to locally increase the temperature to 50 °C/s; a nail penetration device; and an overcharge. The tests were performed in both open and closed setups to analyse the effect of ambient air on gas composition. It was shown that the choice of the trigger method did not significantly affect the amount or composition of gases produced.

### 3.3. Gas Analysis Methods

Gas analysis can be performed continuously to monitor the evolution of gases during venting, or on the total gas volume after venting, is finalised. Continuous monitoring presents a challenge in the experimental design since either optical access or gas sampling must be performed in the vicinity of the vent. The main methods used in the studies reported in this review are listed in Table 2, and the purpose of the present section is to outline the advantages and disadvantages of the methods.

**Table 2.** Gas analysis methods.

Abbrev.	Name	Advantage
FTIR	Fourier Transform Infrared	Non-intrusive detection of a wide range of components
GC	Gas chromatography	Allow the detection and quantification of a wide range of components
GC-MS	GC-mass spectrometry	In addition to GC capability, it includes structural information and is more sensitive
GC-FID	GC-Flame Ionisation Detector	Fast and simple analysis of organic components
OEMS	Online Electrochemical Mass Spectrometry	Allow the online monitoring of selected gases
Raman	-	Non-intrusive detection of a wide range of components
NMR	Nuclear Magnetic Resonance	Give detailed structural information and allow to follow kinetic reactions
IC	Ion Chromatography	Allow the quantification of inorganic F
	Wash bottle	Collection of HF and other inorganic F components

Many of the gas analysis techniques are quite versatile and can be used to detect a wide range of compounds. However, they need to be calibrated to accurately quantify compounds, which means that the researcher needs to know beforehand which compounds to target. It is common to target the components that are expected to occur in large fractions: CO, CO<sub>2</sub>, H<sub>2</sub>, CH<sub>4</sub>, and C<sub>2</sub>-hydrocarbons. Under some conditions, the electrolyte solvent (i.e., carbonates) is also present in significant amounts. This gives important information on the extent of chemical pre-processing that occurs inside the cell before venting since the carbonates are essentially unprocessed battery electrolyte solvent.

Fourier Transform Infrared Spectroscopy (FTIR) is used to identify organic and inorganic materials based on their absorption of infrared light [37]. FTIR works by measuring the interaction of infrared radiation with a sample, providing detailed information about its chemical composition and structure. FTIR has the advantage of being non-intrusive, and it can detect almost all compounds of relevance to LIB vent gases. Depending on the type of FTIR apparatus, it can provide spectra of all compounds in the gas mixture, which allows the identification of minor compounds with, for example, high toxicity.

Gas chromatography (GC) is a widely used analytical technique employed to separate, identify, and quantify the components of complex mixtures [38]. In GC, a gaseous sample is injected into a chromatographic column, where it interacts with a stationary phase. The components of the sample then separate based on their affinity for the stationary phase and their volatility. The species are identified by a detector, often a mass spectrometer when they reach the end of the column. Gas chromatography–mass spectrometry (GC-MS) combines the separation power of gas chromatography with the identification capabilities of mass spectrometry. In GC-MS, the effluent from the GC column is introduced into the mass spectrometer, where the separated components are ionised and fragmented. The resulting mass spectra provide information about the molecular weight and structure of the individual components, allowing for accurate identification and characterisation. LIB vent gas studies employing GC-MS commonly target a range of expected compounds, including CO, CO<sub>2</sub>, H<sub>2</sub>, small hydrocarbons, and O<sub>2</sub>. For accurate quantification, the procedure is calibrated to the target compounds which are identified. There is also a possibility to identify minor compounds in the analysis where the targets are not predefined.

To find the absolute amount of gas formed during a TR experiment, it is common to measure pressure in a known volume and use the ideal gas law to calculate moles of gas [26,39–42].

GC is not suitable for the measurement of hydrogen fluoride (HF) and other fluorinated compounds, but instead, FTIR or wash bottle techniques are used. The wash bottle is conveniently combined with Ion Chromatography (IC) for the quantification of the total amount of fluoride ions in the sample.

The wash bottle technique is a practical method for determining the presence and concentration of HF but has some drawbacks. In a typical setup, a wash bottle containing a solution, often of a calcium salt-like calcium carbonate or calcium sulphate, is used. When HF vapour is present, it reacts with the calcium solution to form a white precipitate of calcium fluoride (CaF<sub>2</sub>). The formation of this precipitate is a direct indication of the presence of HF. Quantitative determination can be achieved by measuring the amount of precipitate formed and relating it to the concentration of HF using stoichiometric calculations. A significant drawback of this method is that if there are other inorganic fluorinated compounds present in the environment that can decompose, hydrolyse, or otherwise react to release HF or fluoride ions, it leads to an overestimation of HF by this method.

#### 4. Component Studies

While the battery cell is a complex system with multiple constituents that may interact in different ways depending on the temperature and chemical environment, it can be advantageous to increase our understanding of the interaction between a few key components. As an example, many studies have investigated only the electrolyte, its decomposition, heat formation, and product formation at various temperatures. Other studies have been

performed on half cells to reveal interactions between the electrolyte and the positive or negative electrode material during thermal events. In the following, extensive but contradictory literature on electrolyte decomposition is reviewed, followed by the more limited literature where cathodes are included. As outlined by, for example, Wang et al. [3], the anode material also plays an important role in the thermal events in LIB. However, the effects of different anode materials on gas composition have not been studied in a systematic way and are, therefore, not reviewed in the present work. For an outline of processes related to the anode, we refer to the work by Du Pasquier et al. [43].

#### 4.1. Electrolyte Decomposition

In this section, the literature on gases originating from only the electrolyte at different conditions is reviewed, including the effect of different carbonates and accelerated degradation due to the Li-salt.

The common electrolytes consist of a mixture of two to four carbonates (commonly including EC, DEC, DMC, EMC, and PC) and Li-salt, which is most often LiPF<sub>6</sub>. The carbonates are flammable and toxic, and the salt and its potential products have varying degrees of toxicity. Understanding electrolyte decomposition is valuable for the evaluation of risks in case of electrolyte leakage during the handling of the battery or pure electrolyte evaporation as a result of mild mechanical abuse where the other cell components are not affected; for example, this includes some of the cases studied by Diaz et al. [44]. However, the full battery system includes several other parts that become chemically active at different temperatures, particularly the electrodes. This means that the reactions and products that are found in studies of electrolyte decomposition alone cannot be expected to mimic conditions in the battery cell. However, a fundamental understanding of the reactivity of the electrolyte is still valuable since it is part of the whole reaction scheme during a thermal event. Electrolyte decomposition may also have implications for the long-term storage of batteries. A study by Fernandes et al. [28] compared the results of electrolyte decomposition investigations to results from the overcharge abuse test of battery cells. They found a qualitative agreement, and from this, they concluded that part of gassing during the overcharge of LIB is a result of electrolyte decomposition. This was not explicitly discussed or shown in any of the other studies but implicitly assumed.

The electrolyte decomposition studies reviewed here include a few [45–49] at conditions similar to normal use or storage conditions at elevated temperatures but below the onset temperature of thermal events. These studies provide insights into the relevance of gassing as part of the ageing of batteries. The studies that target the response of the electrolyte to a thermal event commonly operate by ramping the temperature from ambient up to at least 300 °C, and sometimes as high as 650 °C, while monitoring the heat production and/or the composition of reaction products formed in the liquid or in the gas phase.

At a minimum, the following processes can occur when an electrolyte is heated beyond its point of stability:

1. Chemical reactions in the liquid, producing liquid or gaseous products, or solid residues are formed that may dissolve in the liquid or deposit.
2. The evaporation of the electrolyte.
3. The reaction between gas phase compounds and liquid, potentially generating new gas phase constituents.
4. The thermal decomposition of the electrolyte.
5. Further chemical reactions in the gas phase, between the gas phase electrolyte, electrolyte decomposition products, and gas phase products from the reaction with Li-salt.

Experimental studies on electrolytes may target one or several of the aspects listed above, and discrepancies in the literature can sometimes be attributed to a lack of understanding of which phenomena are studied and the interactions between chemical compounds in different phases.

An overview of the studies related to thermal decomposition and subsequent reactions of the electrolyte is presented in chronological order in Table 3. Here, the discussion of

the literature relates to several issues for which different studies have given different indications: (1) the presence of a direct chemical interaction between the solvent and Li-salt; (2) the effect of water (and other impurities); (3) the extent of formation of fluorinated products; and (4) the presence of an autocatalytic mechanism that contributes to carbonate decomposition. The presence of water or other impurities in the system is a very important factor since it potentially impacts reaction paths and kinetics and thus can lead to several of the noted discrepancies. In addition to these difficulties, mass spectroscopic methods have been reported to potentially have sampling problems with reactive species undergoing side reactions and transforming in the sampling lines or analyser [50], which may affect the results and conclusions.

**Table 3.** Studies of electrolyte decomposition. All cases contain LiPF<sub>6</sub>, if not otherwise stated. Abbreviations in the methods column can be found in Tables 1 and 2.

Study	Electrolyte	Methods	Target Properties
Botte et al. (2001) [51]	EC, DMC	DSC	Thermal stability of liquid, 50–350 °C
Ravdel et al. (2003) [45]	EC, DEC, DMC, EMC	DSC, GC-MS, NMR	Characterisation of decomposition products in liquid and gas phases during heat ramping at 50–300 °C and storage at 85 °C
Gnanaraj et al. (2003) [20]	EC, DEC, DMC	DSC, ARC, NMR	Thermal stability of liquid electrolyte from 40 to 350 °C, and product characterisation in the liquid and gas phase
Campion et al. (2005) [48]	EC, DMC, DEC	NMR, GC-MS, SEC	Mechanistic study of liquid and its gas phase products after storage at 85–100 °C for 1–4 weeks
Kawamura et al. (2006) [47]	EC, DEC, DMC	H <sub>2</sub> O after storage	Rate equation from the reaction of Li-salt with water at 0–30 °C for up to 50 h
Wang et al. (2006) [52]	EC, DEC, DMC, PC	C80-calorimeter	Thermal behaviour during heating to 300 °C, with and without Li-salt
Yang et al. (2006) [46]	EC, EMC, DMC, PC	TGA, FTIR	Characterisation of decomposition products in liquid and gas phases during heat ramping at 50–300 °C and storage at 85 °C
Wilken et al. (2012) [53]	EC, DMC	TGA, FTIR	Characterisation of gas phase products upon the heating of the electrolyte to 300 °C
Lekgoathi et al. (2013) [54]	Only LiPF <sub>6</sub>	TG, FTIR	Mechanistic study of decomposition of Li-salt with and without the presence of water
Wilken et al. (2013) [49]	EC, DMC	Raman, NMR	Gas and liquid characterisation during storage at 85 °C for up to 160 h
Okamoto (2013) [55]	EC	Ab initio calc.	Establish thermal decomposition mechanism in liquid
Yamaki et al. (2015) [56]	PC, EC, DMC	DSC	Determine rate equation during heat ramping to 450 °C
Tebbe et al. (2015) [57]	EC, various Li-Salts: LiPF <sub>6</sub> , LiPOF <sub>4</sub> , LiAsF <sub>6</sub>	DFT calc., liquid phase.	Investigate HF formation from Li-salt decomposition in EC
Lamb et al. (2015) [22]	DMC, EMC, EC, DEC	ARC	Gas production from the thermal decomposition of the solvents with and without Li-salt
Bertilsson et al. (2017) [58]	LP71, EC, PC, DEC, DMC, EA	TG, FTIR.	Emission of gases from solvents and electrolytes are characterised to 650 °C
Solchenbach et al. (2018) [50]	EC	TGA, OEMS	Thermal and oxidative decomposition of LiPF <sub>6</sub> with and without EC to 350 °C
Fernandes et al. (2019) [28]	DMC, EMC, EC, PC	DSC	Thermal degradation of solvents to 300 °C
Liao et al. (2020) [59]	EC, DMC	Auto-clave, GC-MS	Gas emissions from the electrolyte is characterised for heating to 300 °C

An early disagreement in the literature was whether there are direct interactions between the Li-salt or its products with the carbonate solvents. According to the study by Botte et al. [51], there was no evidence of direct chemical interactions between the solvent mixture and LiPF<sub>6</sub> at elevated temperatures, but the presence of the salt lowered the onset temperature for carbonate decomposition. Ravdel et al. [45] used a similar method as Botte et al. but also analysed chemical products and showed that salt decomposes to form phosphorus pentafluoride (PF<sub>5</sub>) and, indeed, reacts with carbonates and other hydrocarbons. At about the same time, Gnanaraj et al. [20] showed that fluorinated hydrocarbons were formed from the interaction of Li-salt with hydrocarbons. However, Yang et al. [46] and Wilken et al. [53] reported that no signs of decomposition products from carbonates were found in their studies.

The presence of water impurities is a factor that has been proposed to strongly affect the products formed in electrolyte decomposition. It is well known that LiPF<sub>6</sub> forms different products with or without water present [54], and the consequences for the electrolyte system have been studied by Kawamura et al. [47] and Campion et al. [48]. At storage conditions, the latter identified fluorophosphate products in the presence of water.

Another controversy concerns the potential catalytic effect of Li-salt and/or its decomposition products on carbonate degeneration, i.e., if compounds like, for example, phosphoryl fluoride (POF<sub>3</sub>) regenerate to further degrade the carbonates.

There are conflicting reports on the importance of and the relative amounts of the reaction products POF<sub>3</sub> and PF<sub>5</sub> related to salt decomposition. While some studies report high concentrations, others report low occurrence or even the absence of these species. In some cases, it has been confirmed that the highly reactive fluorinated species were consumed by side reactions in the apparatus, thus misrepresenting the actual amounts formed [50]. Due to their high reactivity, the accurate quantification of species like HF, PF<sub>5</sub> and POF<sub>3</sub> is challenging and demands precise control of the test setup to avoid the method errors caused by unintended and uncontrolled side reactions with the surfaces in the test equipment.

#### 4.2. Cathode Decomposition

The phrase “battery chemistry” commonly refers to the composition of the cathode material. The chemistry of the LIB cathode varies in performance, cost, and safety due to differences in material composition. The decomposition of the cathode material is a key factor in the internal chemical processing of the battery and the resulting reactivity of vent gases due to the production of O<sub>2</sub> that can initiate or accelerate oxidation processes. The layered oxide cathode materials, such as nickel–manganese–cobalt dioxide (NMC) and nickel–cobalt–aluminium dioxide (NCA), currently used in electric vehicle batteries decompose above the threshold temperatures in the range from about 150 °C to above 300 °C. Cathode material with a high nickel content have a higher specific capacity but poor thermal stability. The onset temperature is mainly a property of the cathode material, but it is, to some extent, also influenced by the chemical (electrolyte composition) and electrical environment. The decomposition mechanisms for different cathode materials and experimental studies reporting on the dependence of the electrolyte composition are comprehensively reviewed by Wang et al. [3] and will not be repeated here. For the analysis in the present work, however, it is relevant to know the thermal reactivity of each cathode material. Lithium–iron phosphate (LFP) cathodes likely produce very little or no oxygen at all, which is represented by the half-cell (cathode) chemistry with the lowest risk going into TR. The reactivity of the oxygen-producing cathodes is ranked as follows: LCO > NCA > NCM > LMO, where LCO and LMO are lithium–cobalt dioxide and lithium–manganese dioxide spinel, respectively. However, it is important to mention that Li-salt decomposition, the breakdown of the SEI and the chemical reactions between the graphite anode and the electrolyte start at lower temperatures than the cathode reactions, typically around 90 °C, but it can be lower [3,19,60]. Consequently, the initial thermal release and gassing are driven by the anode’s side, independently of the cathode. The heat released

from the anode-electrolyte reactions is sufficient to raise the cell temperature to levels where the oxygen-producing cathode materials start to break down.

An important fate of the O<sub>2</sub> released from the cathode is their subsequent reaction with the lithiated anode to produce heat. Oxygen can also react with the carbonates in the electrolyte, producing carbon oxides and hydrocarbons. No significant fraction of O<sub>2</sub> has been reported from studies of vented gases. There are at least two plausible explanations for the low presence of the vented gases: either O<sub>2</sub> is essentially consumed in the chemical reactions inside the cell before the venting occurs, or simply O<sub>2</sub> has not been a target compound for investigation in most studies, and, hence, not measured and reported.

## 5. Experimental Studies of Vent Gases

This section reviews the literature on the composition of vented gases from LIB cells. The criteria for the selection of publications for the analysis are (1) the vented gases have not been ignited, and (2) chemical composition has been determined, including at least the main gases CO, CO<sub>2</sub>, and H<sub>2</sub>. This means that, in this review paper, the focus is on vent gas compositions resulting from the chemical processing in the battery cells only, not gases formed in the combustion reactions outside the cell. A common way to ensure that no combustion occurs is to vent the cells into an inert environment of nitrogen gas. Some studies present results from experiments with and without combustion, and a few are ambiguous on whether combustion took place or not. The current mix of different types of studies found in the literature makes a direct comparison between results challenging and consequent conclusions about the correlation of gas emissions, both in terms of the species detected and their relative amounts, in vent gases as well as the influence of specific test parameters, e.g., SOC, potentially misleading, as will be shown below.

To enable the risk assessment of LIBs, the amount and composition of vent gases must be known, and the aim of this review is to extract information that will allow the fact-based prediction of vent gases, like battery chemistry, SOC, SOH, conditions of thermal event, etc. The studies vary a lot with regard to details reported on the LIB cell properties, the experimental conditions, and the results. Ideally, detailed information about cell material composition is provided; for example, electrode materials, the electrolyte composition, and the relative amounts of ingoing components. Regarding the experiments in detail, it is necessary to disclose the triggering method, as well as the SOC, at the start of the test. The results presented ideally include details on the temperature and heat release, mass loss from the LIB cell, the total amount of gas released, and gas composition including carbonates and fluorinated components. Many publications lack one or more parts of information, which makes it difficult to make comparisons between studies and to draw meaningful conclusions from the results.

The literature is collected and presented in tables in the following sections, with selected information of relevance to gas composition and other important aspects discussed further in the main text. Many studies present the total amount of gases formed, but some distinguish the so-called first vent. The first vent has some interesting characteristics that are outlined in the first subsection.

Comparatively few studies exist on venting following mechanical abuse, and these are found in the second subsection, with comments on the unique aspects related to mechanical abuse. The following sections summarise the works on electrical and thermal abuse, separated into individual tables for each cathode chemistry.

In the tables, the studied cell geometry is given, i.e., pouch, prismatic or cylindrical (Cyl.); among cylindrical cells, the numerals 18650, 26650, etc., refer to cell dimensions with the first two numbers indicating the diameter and the second two the length.

### 5.1. Characteristics of the First Vent

As outlined in the introduction, the thermal and chemical events resulting in gas release from LIBs proceed through a sequence of steps, with several occurring before the onset of what is defined as TR. The time during which the thermal process evolves varies de-

pending on LIB properties and the type and severity of the trigger event. Rapid penetration triggering leads to TR on very short timescales, with no preceding first vent [61]. But for experiments with a moderate heating rate [9,18,35,39,60–62] or gradual overcharging [4,61], gas formation occurs at low temperatures (80–160 °C) and the LIB cell vent and releases a limited volume of gas before the onset of uncontrolled TR. In some cases, the thermal events end with the first vent if the heat produced is effectively dissipated by surrounding materials and no heating above the TR threshold occurs. This has mainly been seen in LFP cells. Characteristic parameters in studies of first-vent events are summarised in Table 4. In all studies, the evolution of the thermal event and overall gas formation were monitored, but the determination of the gas composition of the first vent was not performed in all studies, as noted in the final column.

**Table 4.** Studies where the first vent is detected. If the number of cells is not specified in the second column, the testing was performed on the single-cell level.

	LIB Type	Heating Rate, °C/min	SOC	T at Time of Venting, °C	Gas Volume 1st Vent/Total Volume, %	Main Gaseous Components
Abbott et al. (2022) [63]	NMC Cyl. 18650	~20	5–100	157–125		CH <sub>4</sub>
Essl et al. (2021) [9]	NMC pouch, aged and fresh	2	100	~120	3–7	Gas composition of 1st vent not determined
Essl et al. (2020) [60]	NMC/LMO pouch	0.33–0.39	0, 30, 100	120–130	6	DEC, CO <sub>2</sub> , H <sub>2</sub> O
Essl et al. (2020) [61]	NMC pouch	2	100	121	4	Gas composition of 1st vent not determined
		-	OC	56		
Essl et al. (2020) [61]	NMC prismatic	2	100	138	2	Gas composition of 1st vent not determined
		-	OC	66		
Fernandes et al. (2018) [4]	LFP Cyl. 26650	-	OC	80	0.7	DMC, EMC, C <sub>2</sub> H <sub>4</sub> , CO <sub>2</sub> , CO
Lammer et al. (2018) [18]	NCA Cyl. 18650, aged cells	0.5	100	116–139	2–4	CO <sub>2</sub> , C <sub>2</sub> H <sub>2</sub> (aged), (solvent not monitored)
Lammer et al. (2017) [35]	NCA Cyl. 18650	0.5	100	130	<3	CO <sub>2</sub> (solvent not monitored)
Golubkov et al. (2015) [39]	LFP Cyl. 18650	2	0–100 and OC	130–150 but 80 at OC	-	Gas composition of 1st vent not determined
Golubkov et al. (2014) [62]	NCA Cyl. 18650	2	0–100 and OC	195	~7	Gas composition of 1st vent not determined
	LFP Cyl. 18650	2	0–100 and OC	168	~7	Gas composition of 1st vent not determined
	NMC Cyl. 18650	2	0–100 and OC	149	~7	Gas composition of 1st vent not determined

The first vent can be detected as a pressure or gas volume increase, depending on the nature of the experimental apparatus. While in the majority of gassing studies, gas sampling is performed after the main venting is completed (to determine the composition of all vented gases), there are only a few studies where the gas is continuously monitored using FTIR or regularly sampled to a GC-MS to enable the identification of the main constituents at different times in the venting process [4,18,35,60]. Since the gases in the first vent only comprise the gases formed by chemical processing in the cell before the onset of TR, it is likely that the composition may show similarities to gases formed during the ageing process of the cell, which are mentioned in Section 2 on gases produced during

regular use conditions. Thus, the first vent, as investigated in experimental studies, is potentially useful to increase understanding and predict gases that may be released at the battery's end-of-life. It can also provide complementary information when interpreting TR gas data from aged cells compared to pristine cells, as at least initially, the gases emitted at the onset of TR from aged cells are likely already present in the cell and not as direct products of the TR event itself.

Among the early detection strategies for LIB failure, the detection of CO, CO<sub>2</sub>, and hydrocarbons has been suggested [64]. This strategy relies on the first vent preceding the main vent. Considering the experimental evidence that under some circumstances, the timescale of a TR in real applications is so short that a minor first vent is not detected, such detection strategies cannot be expected to reliably predict every LIB failure beforehand.

The experiments presented in Table 4 include the detection of a first vent, in which the gas volume is in the range of about 1–7% of the total gassing when the first vent was followed by a main vent. When overcharge was used to trigger TR, the venting occurred at or below 80 °C (measured at the surface of the cell). For temperature triggers, the first vent occurred at temperatures from 120 to 195 °C, with the NMC and NCA cells in the lower part of this range. The venting seemed to occur after the onset of SEI breakdown but before the separator melted completely and a full ISC developed in the cell. The internal production of O<sub>2</sub> gas from the cathode material was initiated at higher temperatures and was not expected in the first vents, which was confirmed in the studies that were instrumented to detect O<sub>2</sub> [35,60].

Regarding the identification of the composition of the first vent, all studies in which species detection was performed indicated CO<sub>2</sub> as an important or even dominant species. In the studies by Lammer et al. [18,35], CO<sub>2</sub> was identified as the main constituent, but caution has to be exercised in the interpretation of the results since the apparatus did not allow the detection of carbonate solvents. In the studies where solvents were monitored, carbonates were identified as the main components [4,60]. In the study of cells aged by cycling and storage, Lammer et al. [18] concluded that, while new cells mainly released CO<sub>2</sub> in the first vent, the aged cells had a large share of short hydrocarbons. Calendar-aged cells, in particular, had significant amounts of C<sub>2</sub>H<sub>2</sub>, which was attributed to gases formed during the ageing processes and not in direct response to the experimental trigger.

All studies except one were performed at 100% SOC or higher; however, the only study with a lower SOC indicated that the gas volume of the first vent was not dependent on SOC [60]. In conclusion, the first vent is most likely the outcome of mainly the evaporation of the solvent and decomposition of solvents with low decomposition temperatures.

## 5.2. Mechanical Abuse Tests

The mechanical abuse of EV batteries commonly involves the penetration or deformation of the battery pack by impact. There is a range of mechanical trigger methods used to test batteries, including compression, bending, and penetration [36]. Penetration is considered to be the most severe condition since it results in an instantaneous short circuit [19]. The immediate effects of mechanical abuse on the battery at the cell level can be short-circuiting between the positive and negative electrodes, resulting in the discharge of electrical energy and/or the rupturing of the cell wall, leading to the leakage of the electrolyte. Experimental studies have been conducted to investigate the thermal effects and energy release resulting from mechanical abuse. For an overview of thermal events after mechanical abuse, we refer to Feng et al. [19]. Examples of studies include rapid nail penetration [65], slow nail penetration [66] and abuse with a blunt rod [67]. In the present work, the focus is on the gas release, for which a few experimental studies with nail penetration as the trigger have been performed; these are summarised in Table 5.

The effect of penetration is the instantaneous release of gases [68], but in some laboratory tests, nail penetration has been shown to produce significantly smaller gas volumes compared to thermal abuse [44] or overcharge abuse [61]. However, as noted by Feng et al. [19], the common nail penetration tests show a lack of reproducibility. For nail

penetration setups, the sealing of the nail hole to avoid creating an alternative route for smoke and gas to escape is important as this may impact the internal chemical processing inside the cell and, hence, the gas composition. Sealing information is not always explicitly available in publications and may explain some of the differences in gas compositions between studies.

The most comprehensive gas composition investigations from mechanical abuse are the nail penetration tests by Essl et al. [61]. The tests were performed in a sealed chamber with a nitrogen atmosphere, with a 42CrMo4 nail of 3 mm diameter and cone angle of 60°, pushed 8 mm perpendicularly into the cell. It immediately triggered gas release and heating above 700 °C for both pouch and prismatic cells. There was only one venting, starting when the cell was penetrated. Approximately equal amounts of CO and CO<sub>2</sub> were emitted, based on volume, and close to the same volume of H<sub>2</sub>, with smaller amounts of C<sub>2</sub>H<sub>4</sub>, CH<sub>4</sub>, and H<sub>2</sub>O. From the experimental description, it is not clear whether the venting occurred at the site of penetration or through the cell safety valve (for prismatic cells, pouch cells do not have a dedicated valve).

**Table 5.** Summary of experimental studies targeting vent gases from LIB after nail penetration. If the number of cells is not specified in the second column, the testing was performed on the single-cell level. Gases are listed in order of relative amount, starting with the most abundant compound.

Reference	Type	SOC, %	Electrolyte	Gases	Detection Method
Willstrand et al. (2023) [14]	NMC811 Prismatic	100	-	No gas detection for this trigger method	NDIR, FTIR
Hoelle et al. (2021) [69]	NMC111 Prismatic	100	EC:DMC:EMC 1:1:1	H <sub>2</sub> , CO, CO <sub>2</sub> , C <sub>2</sub> H <sub>4</sub> , CH <sub>4</sub>	GC
Essl et al. (2020) [61]	NMC622 Prismatic	100	EC:EMC 1:1	CO <sub>2</sub> , H <sub>2</sub> , CO, C <sub>2</sub> H <sub>4</sub> , CH <sub>4</sub> , H <sub>2</sub> O	FTIR, GC
	NMC622 Pouch		EC:DMC:EMC 2:3:3	CO <sub>2</sub> , CO, H <sub>2</sub> , C <sub>2</sub> H <sub>4</sub> , CH <sub>4</sub> , H <sub>2</sub> O	
Diaz et al. (2019) [44]	LCO Cyl. 18650	0–100	DEC, DMC, EC, EMC, PC	Carbonates, CO, HF, H <sub>2</sub> O	FTIR online, IC
	NMC Cyl. 18650	100			
	LFP Cyl. 18650	100			
	LCO Pouch	100			
Koch et al. (2018) [68]	NMC Pouch	100	-	Hydrocarbons/CO not specified	Gas sensors
Nedjalkov et al. (2016) [70]	NMC Pouch	>100	EMC, EC	Carbonates, CO, HF, CO <sub>2</sub> , aromatic hydrocarbons	GC-MS, QMS, IC, offline analysis

The study by Diaz et al. [44] included mechanical and thermal (see Section 5.4) abuse mimicking recycling. For nail penetration, several cases showed no TR and only small amounts of gas production. It was concluded that, in these cases, electrolyte boiling off was the main gassing mechanism.

Koch et al. [68] did not give any details on the gas composition but focused on the dynamics of the event. Their aim was to investigate sensors, and the main takeaway for the context of the present review is that they detected gas venting instantaneously at penetration and modest surface temperature increases of about 150 to 300 °C.

Hoelle et al. [69] triggered 50 NMC and NCA cells of various capacities to the TR and found that the vented mass of gas had a linear dependence on cell capacity (Ah). They

only performed vent gas analysis on one NMC cell, which expelled about 30 vol% each of CO, CO<sub>2</sub> and H<sub>2</sub>, respectively. The remaining 10% consisted of nearly equal amounts of the small hydrocarbons CH<sub>4</sub> and C<sub>2</sub>H<sub>4</sub>, which seems reasonable, considering that the electrolyte solvent contained similar amounts of methyl and ethyl groups.

Since the data are scarce, no significant trends were revealed, but one observation worth mentioning is that high temperatures were not reached in a majority of the tests. In the studies by Diaz et al. [44] and Nedjalkov et al. [70], carbonates and other large hydrocarbon fragments were detected, which indicated limited chemical processing in the battery before gas release. The gases are, for the most part, evaporated electrolytes. The study by Nedjalkov et al. [70] is the only one monitoring the release of heavier hydrocarbons, for example, benzene, and is relevant for the assessment of toxicity.

To understand the gas composition resulting from pure mechanical abuse, more experimental data are needed. The thermal effects of mechanical abuse were strongly dependent on the surroundings, for example, if the triggered cell was part of a battery pack. The mechanical abuse resulted in heat and gas release, and if the heat was not dissipated in the system, it triggered further heating and a full-scale TR event, which could propagate to surrounding cells in the case of a battery pack.

### 5.3. Electrical Abuse Tests

Overcharging is a severe form of abuse where the cell is forced into abnormal electrochemical conditions, and the battery is filled with excess electrical energy, which normally is not present and needs to be consumed. This triggers exothermic side reactions and results in the decomposition of cell materials, producing gases [19]. Minor overcharge conditions contribute to accelerated ageing, whereas more extensive overcharge leads to immediate cell failure. In EVs and battery installations with a well-designed battery management system, electrical abuse conditions, such as overcharge, overcurrent, and over-discharge, are effectively prevented, and for EVs, effective protection against electrical abuse is part of globally regulated safety requirements for homologation [71].

Over-discharge leads to the over-delithiation of the anode, the decomposition of the SEI, and the production of CO and CO<sub>2</sub> [19]. This will induce increased pressure, cell swelling, and a changed chemical environment in the cell, which will influence subsequent chemical processes.

Experimental studies reporting gas composition from overcharged LIB cells are summarised in Table 6. To the best of the authors' knowledge, there is no published report on gas composition analysis as a result of the over-discharge TR trigger.

**Table 6.** The summary of experimental studies targeting vent gases from Li-ion batteries after overcharge. If the number of cells is not specified in the second column, the testing was performed on single-cell level.

Reference	Cathode	SOC, %	Electrolyte	Gases	Detection Method
Willstrand et al. (2023) [14]	NMC811 Prismatic	128, 131	-		NDIR, FTIR
Cai et al. (2021) [64]	NMC Prismatic	213	-	CO <sub>2</sub>	Gas sensor
Yuan et al. (2015) [72]	NMC Prismatic	100–200	-	CO, CO <sub>2</sub> , CH <sub>4</sub> , C <sub>2</sub> H <sub>4</sub> , C <sub>2</sub> H <sub>6</sub>	GC-MS
Essl et al. (2020) [61]	NMC622 Prismatic	147	EC:EMC 1:1	CO, CO <sub>2</sub> , H <sub>2</sub> , CH <sub>4</sub> , C <sub>2</sub> H <sub>4</sub> , H <sub>2</sub> O	FTIR, GC
	NMC622 Pouch	146	EC:DMC:EMC 2:3:3		

#### 5.4. Thermal Abuse Tests

As mentioned in Section 3.1, slow and uniform heating is the most commonly used among the thermal abuse trigger methods, but there are a few studies that use localised and/or rapid heating. Appropriate information about the heating method and rate is given in the summary tables when such data are provided in the original publication.

This section is organised with subsections for different cathode chemistries, and the vent gas experiments are summarised in tables. Please note that the focus is on relative gas composition. All studies report on increasing absolute gas amounts with increasing SOC, but the focus of our analysis is on the relative amounts since it defines the flammability and explosion characteristics of the gas mixtures.

Some experimental data are plotted in figures to enable the discussion of trends. Cathode chemistry and SOC are the two factors generally considered to determine gas volume and composition. However, it is highly likely that gas composition is also dependent on other cell properties like the electrolyte composition and external factors, such as the amount of added energy transferred to the LIB cell during the abuse testing. Cell geometry (prismatic, pouch, cylindrical) may also play an important role since heat transfer and dynamics can vary depending on cell geometry and size.

##### 5.4.1. LFP Batteries

Lithium–Iron Phosphate (LFP) batteries are claimed to represent a superior safety profile, long cycle life, and stable thermal characteristics compared to cells with layered oxide cathode materials, such as NMC and NCA. This is due to the chemical stability of the olivine structure. Unfortunately, LFP offers a lower energy density compared to other lithium-ion chemistries, but thanks to their long cycle life with many charge–discharge cycles, they are suitable for applications in electric vehicles, renewable energy storage, and grid stabilisation.

Experimental studies reporting on vent gases from LFP cells are collected in Table 7, and major gaseous components are plotted in Figures 2 and 3. All plotted data are for cylindrical cells with relatively low capacity, which means it is a fairly homogeneous dataset. However, heating has been conducted with different methods and heating rates, which may result in different dynamics and, therefore, also different gas production.

**Table 7.** Vent gas studies targeting LFP batteries. If the number of cells is not specified in the second column, the testing was performed on single-cell level.

Reference	Cell Geometry	Capacity, Ah	Electrolyte	SOC, %	Abuse Condition	Detection Method
Yang et al. (2023) [73]	Cyl 18650	1.5	DMC:EMC 1:1.9			
		1.1	DMC:EMC:EC 1.9:2.8:1			
		1.8	DMC:EMC:EC 1:1.9:1.4	25, 50, 75, 100	Electric heater, 19 W	GC, GC-FID
		1.1	DMC:EMC:EC 1.0:2.8:1			
Robles and Jeevarajan (2020) [74]	Cyl	5.5	DMC, EMC, ratio unknown	100	10 °C/min	FTIR, GC-MS
Yuan et al. (2020) [26]	Cyl 26650	3.8	-	100	ARC: 4.9 kW DSC: 10 °C/min	GC
Sturk et al. (2019) [75]	5 pouch cells	7	-	100	Heating (rate not given)	FTIR
Gully (2019) [76]	Cyl. 26650	1.5 2.5	-	50, 75, 100, OC	Heating (rate not given)	FTIR

**Table 7.** Cont.

Reference	Cell Geometry	Capacity, Ah	Electrolyte	SOC, %	Abuse Condition	Detection Method
Diaz et al. (2019) [44]	Cyl. 18650	1.1	DEC, DMC, EMC, PC. Ratios not known.	100	Heating (rate not given)	FTIR
Maloney (2016) [77]	Cyl. 26650	-	-	100	Heating (rate not given)	NDIR (CO, CO <sub>2</sub> ), GC-FID (THC), O <sub>2</sub> detection
Bergström et al. (2015) [78]	Pouch	-	-	-	Heating (rate not given)	GC-MS
Golubkov et al. (2015) [39]	Cyl. 18650	1.1	DMC, EMC, EC, PC, MPC	0, 50, 100, OC	Heating (rate not given)	GC
Golubkov et al. (2014) [62]	Cyl. 18650	1.1	DMC:EMC:EC:PC, 4:2:3:1	100	Heating, 1.5–3.5 °C/min	GC-MS

A clear trend seen in Figure 2 is that CO concentrations are low, below 10% for most cases, including both inert and air environments. There is no significant increase in CO with increasing SOC. CO<sub>2</sub> concentrations, as well as H<sub>2</sub> concentrations (Figure 3), are greatly scattered between the datasets, but within each dataset, the trend is decreasing CO<sub>2</sub> with increasing SOC. The hydrocarbons are generally below 20%, but for the few datasets with a higher hydrocarbon fraction, the CO and CO<sub>2</sub> levels are low, indicating a limited chemical oxidation.

Among the studies listed in Table 7, the ones by Golubkov et al. [39,62] are considered the most reliable in terms of gas composition due to the use of a good experimental design in an inert environment.

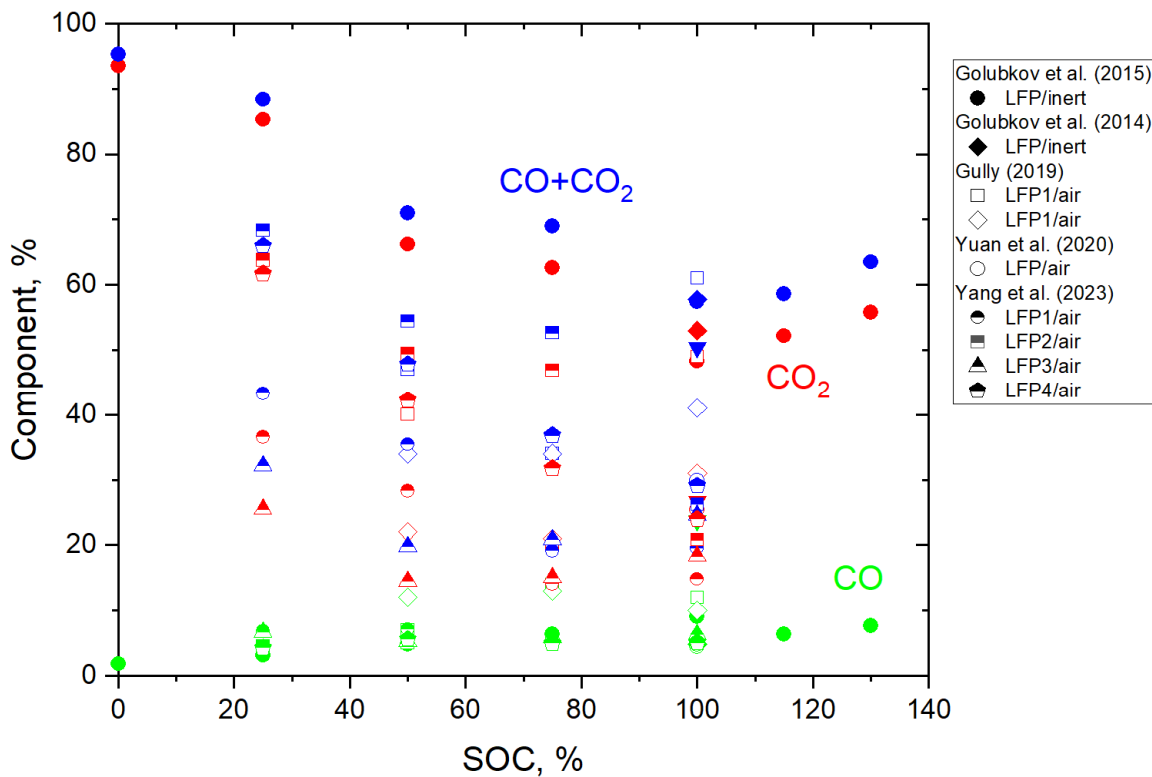


**Figure 2.** Fraction of CO and CO<sub>2</sub>, and the sum of the two, vs. SOC for LFP cells. Filled symbols represent experiments performed in an inert environment. (The mentioned references are Golubkov et al. [39,62]; Gully [76]; Yuan et al. [26]; Yang et al. [73]).

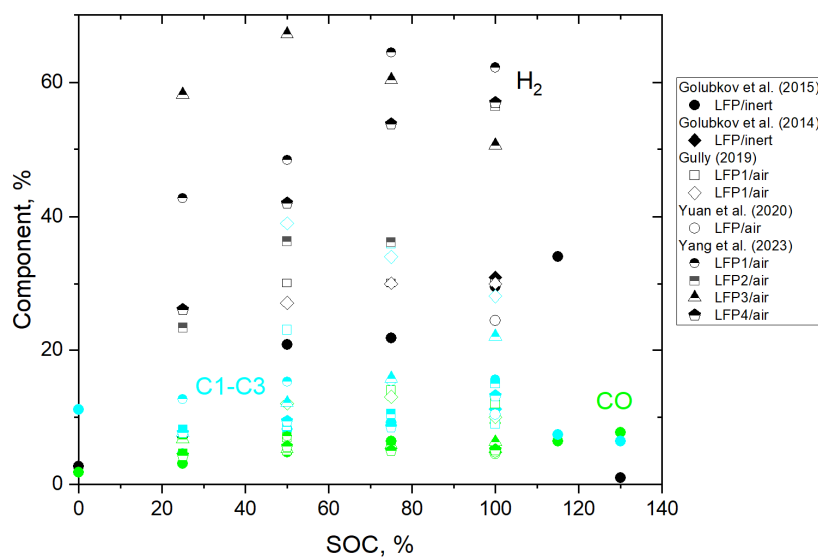


**Figure 3.** Fractions of CO and  $\text{H}_2$ , and the sum of C<sub>1</sub>–C<sub>3</sub> hydrocarbons, vs. SOC for LFP cells. Filled symbols represent experiments performed in an inert environment. (The mentioned references are Golubkov et al. [39,62]; Gully [76]; Yuan et al. [26]; Yang et al. [73]).

#### 5.4.2. NMC Batteries

Nickel–Manganese–Cobalt (NMC) batteries are used in applications requiring a balance of power and longevity and higher energy densities compared to LFP batteries. This makes NMC batteries particularly suitable for EVs and portable electronics, where energy density and performance are critical. NMC cells are quite well studied, as evident from Table 8, where the vent gas studies are collected. Studies have been performed on cylindrical, prismatic, and pouch cells over a wide range of capacities.

**Table 8.** Vent gas studies targeting NMC batteries. If the number of cells is not specified in the second column the testing was performed on the single-cell level.

Reference	Cell Geometry	Capacity, Ah	Electrolyte	SOC, %	Abuse Condition	Detection Method
Zhang et al. (2024) [79]	Cyl 18650	2.5	DEC:EMC:EC	30, 50, 70, 100, 120	Heating/ARC, rate not specified	GC-FID
	Prismatic	157	-	25, 50, 75, 100	Uniform heating, 1 °C/min	
Willstrand et al. (2023) [14]	Prismatic	157	-	50, 100	Uniform heating, 20 °C/min	Off-line analysis with NDIR, GC
	Prismatic	157	-	100	Local heater, rate not specified	
	Prismatic	157	-	>100	Overcharge	
Amano et al. (2023) [80]	Pouch	2.5	EC:DMC:DEC:EMC	30–100		FTIR
Amano et al. (2022) [81]	Pouch	10 10, 32	DMC:EC:EMC:PC	30–100	Heating plug, rate not specified	FTIR
					Heating plate, rate not specified	
Abbott et al. (2022) [63]	Cyl 21700	5	-	25, 100	Heating ~20 °C/min	MS. Gas analyser CO
Essl et al. (2021) [9]	Pouch	60	EC:EMC 1:1	100	Heating, rate not specified	FTIR
Cai et al. (2021) [64]	Prismatic	-	-	0–213	Heating, rate not specified	NDIR, only CO <sub>2</sub>

**Table 8.** Cont.

Reference	Cell Geometry	Capacity, Ah	Electrolyte	SOC, %	Abuse Condition	Detection Method
Robles and Jeevarajan (2020) [74]	Prismatic	25	DMC, EMC, proportions unknown	100	Heating, 10 °C/min	FTIR, GC-MS
Yuan et al. (2020) [26]	Cyl. 18650	3.2	-	100	ARC: 4.9 kW DSC: 10 °C/min	GC
Essl et al. (2020) [61]	Pouch	60	EC:EMC 1:1	100	Heating, 2 °C/min	FTIR, GC
	Prismatic	60	EC:DMC:EMC 2:3:3	100	Heating, 2 °C/min	FTIR, GC
Chen et al. (2020) [82]	5 Cyl. 18650	-	-	60, 100	Uniform heating, rate not specified	GC-MS
	7 Cyl. 18650	-	-	100		
Gully (2019) [76]	Pouch	63	-	50–100, overcharge	Heating, rate not specified	FTIR
Diaz et al. (2019) [44]	Cyl. 18650	2.6	DEC, DMC, EMC, PC	100	Heating, rate not specified	FTIR
Koch et al. [68]	41 Pouch 10 Prismatic	20–81	EC, DMC, DEC, EMC	100	Heating, 1 °C/min	GC-WLD
Bergström et al. (2015) [78]	Pouch	-	-	-	Heating, rate not specified	GC-MS
Golubkov et al. (2014) [62]	Cyl. 18650	1.5	DMC:EMC:EC:PC, 7:1:1:1	100	Heating 2 °C/min	GC
Maloney (2016) [77]	Cyl. 26650	-	-	100	Heating, rate not given	NDIR (CO, CO <sub>2</sub> ), GC-FID (THC), O <sub>2</sub> detection

Figures 4 and 5 include data from studies covering a range of SOCs for CO/CO<sub>2</sub> and CO/H<sub>2</sub>/C1–C3, respectively. A general trend is increasing concentrations of reactive components and decreasing concentrations in CO<sub>2</sub> with increasing SOC. The capacity of the prismatic LIB cell studied by Willstrand et al. [14] was more than an order of magnitude larger than that of the cylindrical cells studied by Zhang et al. [79] and Abbott et al. [63].

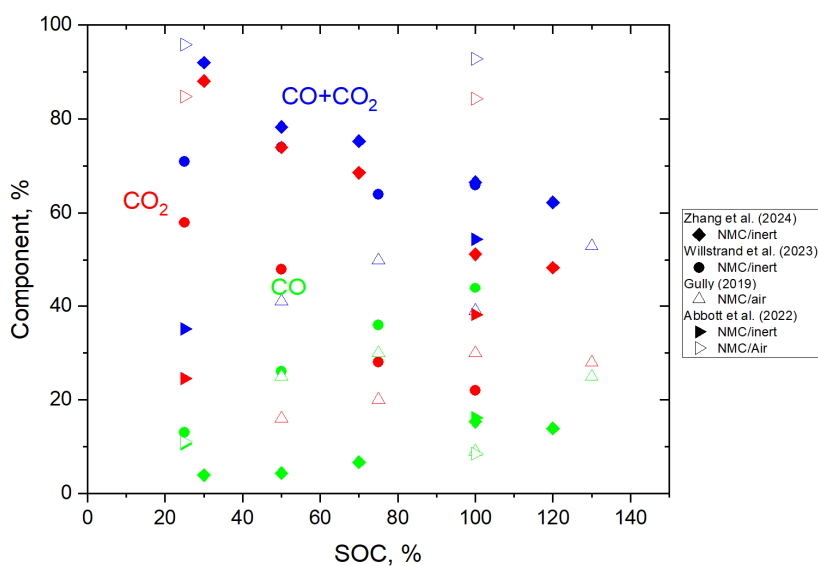


**Figure 4.** Fractions of CO and CO<sub>2</sub>, and the sum of the two vs. SOC for NMC cells. Filled symbols represent experiments performed in an inert environment. (The mentioned references are Zhang et al. [79]; Willstrand et al. [14]; Gully [76]; Abbott et al. [63]).

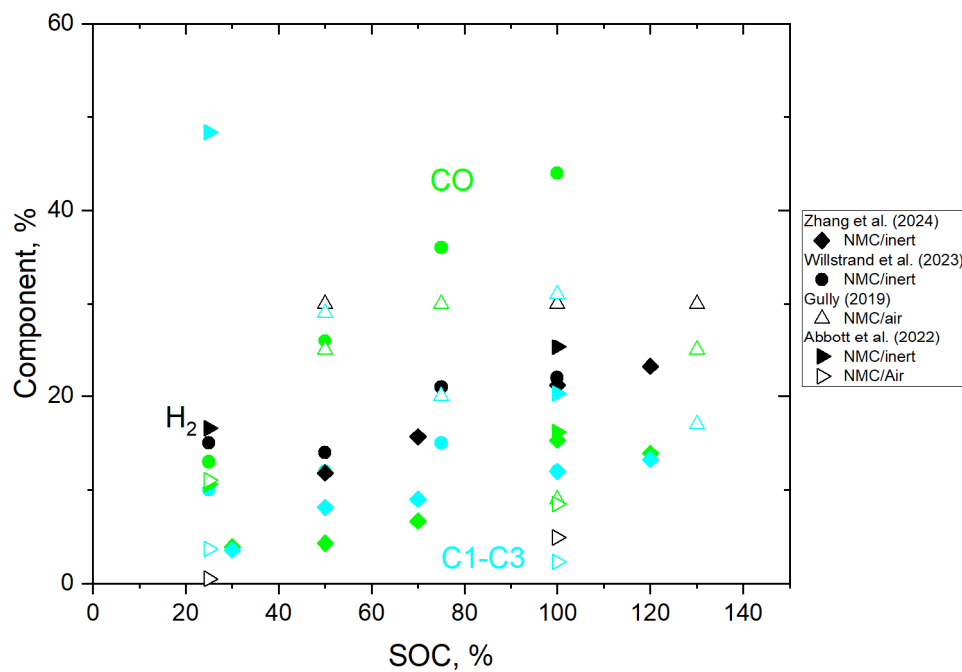


**Figure 5.** Fractions of CO and H<sub>2</sub>, and the sum of C1–C3 hydrocarbons vs. SOC for NMC cells. Filled symbols represent experiments performed in an inert environment. (The mentioned references are Zhang et al. [79]; Willstrand et al. [14]; Gully [76]; Abbott et al. [63]).

While most works focus on major constituents, the study by Diaz et al. [44] focused on toxic gases and is, therefore, valuable for the interpretation of toxicity based on minor substances. The toxic components detected were DC, EC, PC, DMC, HCl, CO, Acrolein, COF<sub>2</sub>, HF, and formaldehyde.

#### 5.4.3. NCA Batteries

NCA batteries have a high specific energy and are common in high-performance applications, particularly in premium EVs and aerospace technologies, due to their excellent energy density and durability. NCA LIB cells have been studied less than LFP and NMC cells, and as seen in Table 9, the only cell geometry studied is cylindrical 18650 cells with relatively low capacity. Heating in these experimental studies has been uniform and at a moderate rate, which indicates that the results may be comparable. Also, all studies employed GC techniques for gas measurements of CO, CO<sub>2</sub>, H<sub>2</sub>, and small hydrocarbons of CH<sub>4</sub>, C<sub>2</sub>H<sub>4</sub>, and C<sub>2</sub>H<sub>6</sub>, but excluding electrolyte species. Several studies targeted the detection of O<sub>2</sub>, but it was not found.

The first two studies, published in 2004 and 2006 by Crafts et al. [83] and Abraham et al. [27], respectively, reported experiments where the cells were heated to 150 or 160 °C and then gas samples were extracted. Abraham et al. reported that for an NCA cell subject to slow heating, self-heating started at 84 °C. They allowed heating to proceed up to about 150 °C, then quenched the cells and investigated gas composition and structural changes in the cell materials. Details on the structural changes are outside the scope of the present work but are valuable. Measurements were performed on gases that were extracted from swelled, non-ruptured cells and on the gases that were vented to the atmosphere. The non-vented gas had a significantly higher CO content, which could indicate that, for the vented gases, CO<sub>2</sub> was produced from CO and was further oxidised as the gas came in contact with ambient air. Another finding was that there was quite a large difference between cells quenched at 150 °C and 160 °C; the additional 10 °C led to more than a doubling of the gas volume, indicating that significant internal processing occurred in the cell at this temperature.

The later studies in Table 9 allowed heating to higher temperatures, and the cells went into TR. The experimental setups were designed to maintain an inert atmosphere, which prevented the hot gases from combusting upon venting. Golubkov et al. [39] covered the widest range of SOC, including overcharge.

**Table 9.** Vent gas studies targeting NCA batteries. If the number of cells is not specified in the second column, the testing was performed on the single-cell level.

Reference	Cell Geometry	Capacity, Ah	Electrolyte	SOC, %	Abuse Condition	Detection Method
Abbott et al. (2023) [84]	Cyl. 18650	~3	-	100	Heating, rate not specified, ARC	GC-MS, inert and air atm.
Lammer et al. (2018) [18]	Cyl. 18650	3.35, 2.5	-	100	Heating, 0.5 °C/min, furnace	GC
Lammer et al. (2017) [35]	Cyl 18650	3.2, 3.5	-	100	Heating, 0.5 °C/min, furnace	GC
Golubkov et al. (2015) [39]	Cyl 18650	3.35	DMC, EMC, EC, PC, MPC	0–100, OC	Heating, rate not specified	GC
Abraham et al. (2006) [27]	Cyl 18650	~1	EC:EMC 3:7 (wt)	100	Heat to 150 °C, ~0.02 °C/min, ARC	GC-MS Not inert atm.
Crafts et al. (2004) [83]	Cyl 18650	1.1	EC:EMC 3:7 (wt)	60, 100	Heating, 0.02 °C/min, ARC	GC-MS Not inert atm.

Two studies were published by Lammer et al. in 2017 [35] and 2018 [18]. In the later study, they investigated three NCA batteries with different characteristics that gave different gas compositions. Lammer et al. [18] argued that there are differences in other properties, like separator material and thickness, that could affect the gas composition, but the effects of these factors have not been studied. The gases expelled at TR are more similar for the different NCA cells compared to an NMC cell from the same study and contain high levels of H<sub>2</sub> and CO.

Figure 6 presents CO and CO<sub>2</sub> concentrations and the sum of the two for the studies on NCA cells listed in Table 9. The study by Golubkov et al. [39] is the only one covering the full range of SOCs. This study is of high quality with good experimental design and excellent characterisation of important aspects of the experiment and is, thus, considered reliable. An important trend was that at a low SOC, CO<sub>2</sub> dominated, while CO increased and dominated at a SOC greater than 60%. However, the sum of the CO and CO<sub>2</sub> was consistent at about 70% for all cells. The other studies performed in an inert atmosphere, all at SOC 100%, showed some scattering but no clear deviation from the relationship between CO and CO<sub>2</sub>. Figure 7 represents flammable components, including CO, H<sub>2</sub>, and the sum of C1–C3 hydrocarbons for the studies in Table 9. Here, the results produced in an inert atmosphere are in quite good agreement, while the ones in the air deviate. The difference between studies in an air environment can likely be attributed to the fact that there were various amounts of oxidiser present and different time scales for the oxidation chemistry to take place. The extent of external oxidation will depend on the volume of air that the vent gases are expanded into and the time before the measurement is conducted. Also, the dynamics of the venting process may be affected since the entrainment of the air into the venting plume can result in a different extent of oxidation.

#### 5.4.4. NMC/LMO Batteries

Nickel–Manganese–Cobalt oxide/Lithium–Manganese oxide (NMC/LMO) batteries are a hybrid type of LIB that combines the advantages of both NMC and LMO chemistries. By blending these two materials, the battery benefits from the high energy density of NMC and the safety and stability of LMO. The two available studies are summarised in Table 10.

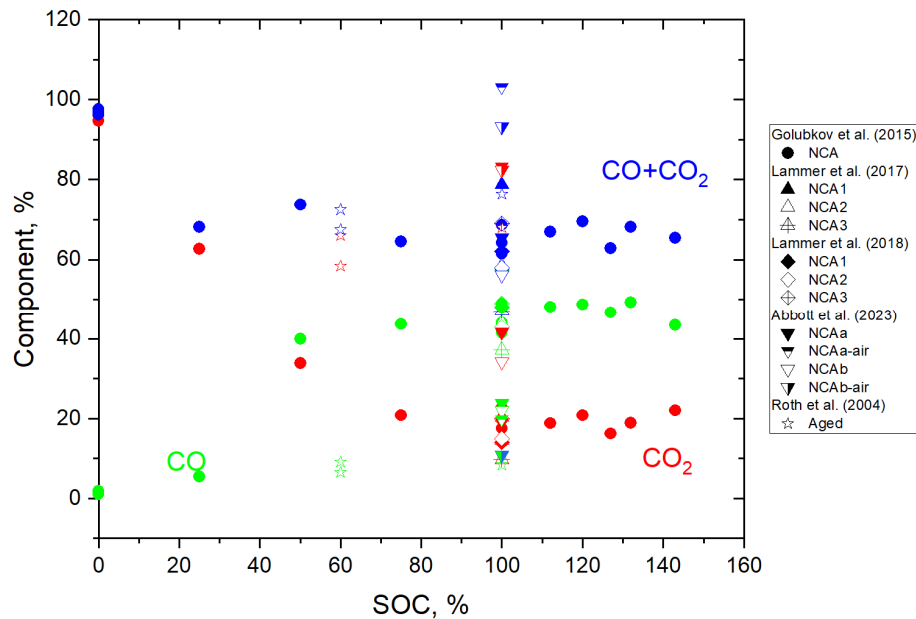


**Figure 6.** Fraction of CO and  $\text{CO}_2$ , and the sum of the two vs. SOC for NCA cells. (The mentioned references are Golubkov et al. [39]; Lammer et al. [18,35]; Abbott et al. [84]; Roth et al. [24]).

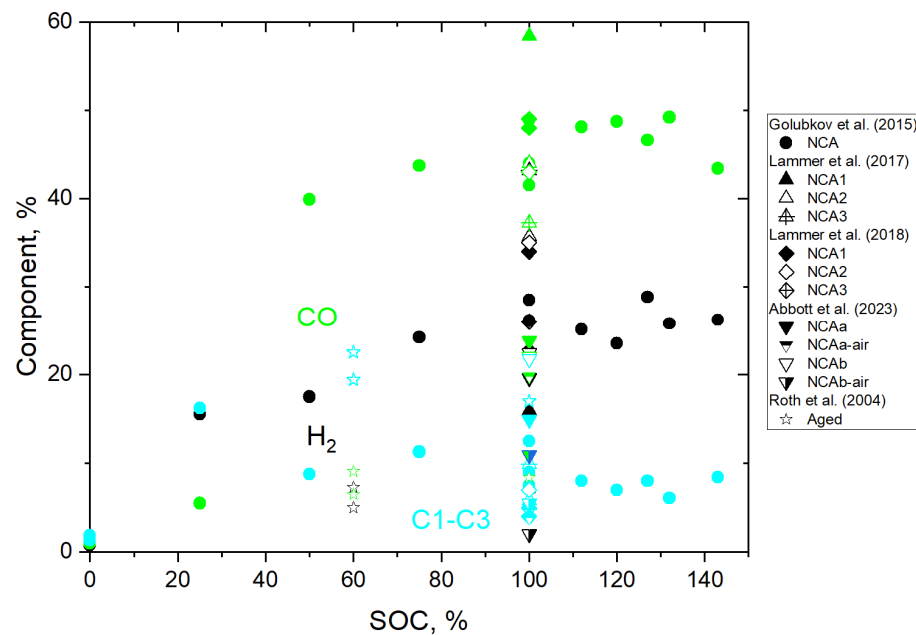


**Figure 7.** Fraction of CO and  $\text{H}_2$ , and the sum C1–C3 hydrocarbons vs. SOC for NCA cells. (The mentioned references are Golubkov et al. [39]; Lammer et al. [18,35]; Abbott et al. [84]; Roth et al. [24]).

**Table 10.** Vent gas studies targeting NMC/LMO batteries. If the number of cells is not specified in the second column, the testing was performed on the single-cell level.

Reference	Cell Geometry	Capacity, Ah	Electrolyte	SOC, %	Abuse Condition	Detection Method
Sturk et al. (2019) [75]	5 pouches	14	-	100	Heating, rate not specified	FTIR
Essl et al. [60]	Pouch	41	EC:DEC:DMC 48:48:4	100, 30, 0	Heating, rate not specified	FTIR, GC

The study by Essl et al. [60] on pouch cells was also conducted in an inert environment and gave a low relative concentration of CO compared to studies on other battery chemistries. Also, low H<sub>2</sub> fractions were detected by Essl et al. [60]. The study seemed to be well-designed and may be an indicator that NMC/LMO vent gases are relatively harmless. However, more studies are needed to establish this trend.

Sturk et al. [75] detected only the components HF and CO<sub>2</sub>, but is a valuable contribution to the understanding of the dynamics of venting.

#### 5.4.5. LCO Batteries

Lithium–Cobalt oxide (LCO) batteries are one of the earliest and most widely used types of LIB, particularly in consumer electronics like smartphones, laptops, and cameras. The cathode material in LCO batteries is composed of cobalt oxide, which provides a high energy density, allowing for compact and lightweight battery designs with substantial energy storage.

Even though LCO batteries are widely used, there are few studies dedicated to the determination of gas composition resulting from thermal abuse. The three available studies are summarised in Table 11.

**Table 11.** Vent gas studies targeting LCO batteries. If the number of cells is not specified in the second column, the testing was performed on the single-cell level.

Reference	Cell Geometry	Capacity, Ah	Electrolyte	SOC, %	Abuse Condition	Detection Method
Kennedy et al. (2021) [85]	Pouch	10	EC:DMC, 1:1	50, 75, 100	Fast uniform heating	GC-TCD
	5 Pouches	10		50, 75, 100		
	5 Pouches	18.5		100		
Diaz et al. (2019) [44]	Cyl. 18650	3	DEC, DMC, EMC, PC. Ratios not known.	0, 50, 100	Uniform heating (rate not stated)	FTIR
	Pouch	2.5		100		FTIR
Maloney (2016) [77]	Cyl. 18650	2.6	-	10–100	Uniform heating (rate not stated)	NDIR (CO, CO <sub>2</sub> ), GC-FID (THC), O <sub>2</sub> detection

The studies by Maloney [77] and Diaz et al. [44] both include cylindrical LIBs with similar capacity and covering a range of SOCs, but apart from that, the information from the publications is quite different with Diaz et al. focusing on toxic products and Maloney on combustible gases. Maloney saw a rather constant THC (total hydrocarbon) level throughout, while the concentrations of combustible CO and H<sub>2</sub> increased from about 40 and 60% SOC, respectively. A weakness in this study is that the quantified gases (CO, CO<sub>2</sub>, H<sub>2</sub>, THC) only add up in the range of 20 to 80% of the total gas volume, which means there is a large number of other gas species that were not identified. This, in combination with a lack of information on the LIB cell and experimental procedure, limited the use of the data for the assessment of gas composition from LCO batteries.

The recent work by Kennedy et al. [85] focused on the quantification of the gas release rate, but they also reported on gas composition for several SOCs. This is a well-designed study that characterises the LIB cell composition and experiments both on single pouch cells and arrays of five cells. Overall, there were no large differences in the relative concentrations of the measured components (CO, CO<sub>2</sub>, H<sub>2</sub> and small hydrocarbons) over the studied range of SOC. In comparison to other cell chemistries, the authors commented on the fact that they measured lower CO and higher CO<sub>2</sub>, but this may be a result of the fact that they performed the measurements in an air environment while comparing them to studies in an inert atmosphere.

The study by Kennedy et al. [85] is recommended as the best available study on LCO LIB, including valuable results and discussion on the differences between single cells and

arrays. However, since the data on gas composition from venting LCO cells is so scarce, no conclusions can be made on potential differences compared to other cell chemistries.

## 6. Discussion

In this section, selected topics of relevance for the assessment of the quality of vent gas studies are discussed.

### 6.1. Influence of Gas Analysis Methods

The most common gas analysis techniques to study vent gases from LIB are FTIR and GC, with the latter often used in combination with mass spectrometry. A common characteristic of these methods is that they can be used for the screening of all hydrocarbons and many other relevant components. Characterisation, including minor constituents like benzene, toluene, and styrene, has been performed by Nedjalkov et al. [70], Gully [76], and Zhang et al. [42], and including amines and nitriles by Sun et al. [86].

For the assessment of fire and explosion risks, it is sufficient to detect major products of CO, CO<sub>2</sub>, H<sub>2</sub>, and small hydrocarbons. In some cases, electrolytes and other oxygenated hydrocarbons are also relevant if they are present in quantities around a few percent of the total gas volume or more. It is most common to present the gas composition as a percentage of the total gas volume. This introduces a potential source of error if all major constituents are undetected. It is, for example, plausible that the electrolyte solvent was indeed a significant contributor to the total gas volume in a few studies where it was not monitored. If this is true, the presented results indicate too-high concentrations of the reported components. When evaluating the results, it is, therefore, important to understand how the reported percentages are derived, if they build on a true quantification, or are just a presentation of the relative amounts of the selected components that were measured in a specific experiment.

Although HF is not the focus of the present review, it is still relevant to comment on the challenges in accurately detecting and quantifying this compound [87] and, indeed, all reactive fluorinated compounds. Independent of the analysis method, the first challenge was the sampling distance or sampling time and the potential for interactions between the reactive compound and the sampling system. In studies where HF was targeted but undetected, it was likely that it was absorbed on surfaces or was converted to a more stable compound in the sampling system [22,75]. An unexpectedly low HF concentration was, thus, likely a result of the removal of HF in the system. The over-prediction of HF can also occur, for example when the wash bottle technique is used, due to the fact that all F<sup>-</sup>, i.e., inorganic fluorine, will form a precipitate. Therefore, wash bottle results should be interpreted as “total inorganic F” [75]. The accurate determination of HF can be performed in situ using, for example, FTIR detection. But, as discussed by Sturk et al. [75], FTIR results can also be erroneous if it is performed offline. The spread in data, by several orders of magnitude, presented in the review of HF concentrations by Bugryniec et al. [8] is likely a result of both the over- and underestimation, as explained above.

### 6.2. Presence of O<sub>2</sub> in the Vented Gases

As outlined previously, O<sub>2</sub> is produced during the decomposition of cathode material of most LIB types at temperatures in the vicinity of the threshold temperature for TR. It has been speculated that oxygen escaping in the vent gases will sustain a flame, which can be tested by simply calculating the amount of oxygen needed to combust the different gases potentially vented.

Golubkov et al. [39] used a simplified calculation to establish that about 6% of the produced gas volume from the cathode material of an over-charged NCA cell can be O<sub>2</sub>. Based on reaction kinetics, an amount this small will be completely consumed by chemical reactions inside the LIB cell. Possible reaction paths for oxygen produced inside the cell can be to react with the lithiated anode, resulting in significant heat production and a range of reactions with the electrolyte solvents [3].

$O_2$  has been a target component in several experimental studies of vent gas composition using GC [39,60–62] but was not detected. A few percent of  $O_2$  was measured in vent gases from a single LCO cell at 100% SOC but not from an array of five cells in the same study under similar conditions [85]. The authors suggest that the time frame for internal chemical processing is shorter in the single cell since it cools faster; therefore,  $O_2$  escape unreacted.

Willstrand et al. [88] performed a series of tests where  $O_2$  was measured for 70 Ah and 157 Ah cells at 75% and 100% SOC, where two cases were triggered by a slow heating ramp and the rest used a rapid trigger method. The cells that were brought to TR by slow heating did not show  $O_2$  in the vented gases. The cells that were triggered by a rapid trigger method released measurable amounts of  $O_2$ . The lower capacity (70 Ah) of cells had 3–6%  $O_2$  in the vent gases when the SOC was 75%, but for both the fully charged 70 Ah cells and the high capacity (157 Ah) cell at 75%, the concentrations were about 1% or less.

To summarise, the majority of the published gas studies show that no oxygen is vented from LIB cells, and the theoretical analysis of the reaction chemistry strongly suggests that the oxygen is consumed before venting. The few experiments that indeed have  $O_2$  in the vent gas are for single cells with relatively low capacities and at a lower SOC. The described cases have a common denominator in that the temperature after TR triggering is lower and, thus, the internal chemical processing is slower. In the case of a real EV field fire, the scenario is similar to the laboratory cases where no oxygen was detected compared to the ones where oxygen was detected. Furthermore, based on a pure combustion consideration, even the highest amount of oxygen that was detected, about 6%, cannot realistically be expected to sustain a fire. It can, therefore, be concluded that it is very unlikely that LIB fires can be sustained by the internally released oxygen present in the gas mixture and that open flame fire relies on the availability of atmospheric oxygen. However, the oxygen produced by the cell may be sufficient to feed a low-intensity smouldering that may flare up if and when ambient oxygen from the atmosphere becomes available.

### 6.3. The Potential Role of Solvent Composition

Carbonates commonly used as electrolyte solvents differ in important properties like boiling temperature, decomposition temperature, and combustion characteristics. When it comes to combustion, it is also worth noting that the oxygen present in the carbonate molecules can act as oxidisers without having to first form  $O_2$  and that the carbonates are generally combustible at lower external oxygen concentrations compared to hydrocarbons. A number of papers have reported the flammability limits [89,90], ignition delay time [91] and laminar flame speeds [92,93] of relevant carbonates. These works are important when attempting to assess the risk related to the leakage of carbonates as a result of cell punctures, electrolyte spills during manufacturing, or when handling end-of-life LIBs, for example, during recycling. However, to understand the processes occurring during internal chemical processing in an LIB cell during a thermal event, understanding the evaporation and decomposition conditions of the electrolyte solution is more important. In addition, chemical reactions of carbonates with other cell components or their products following decomposition drive exothermic chemistry, resulting in excess heat production during a thermal event.

The boiling points for the common carbonates at ambient conditions are in the range from 91 °C for the smallest carbonate DMC to 248 °C for the cyclic EC [94]. The expected environment inside an LIB cell is different from the ambient, which impacts the electrolyte solvent characteristics. For example, the pressure inside the cell is higher inside the cell and slowly increases due to normal ageing, which will shift the boiling temperature to higher values, whereas the presence of Li-salt may decrease the stability and initiate decomposition at lower temperatures than ambient temperatures. However, the trends in boiling point and stability are still relevant to consider. A mild thermal event can start at a temperature as low as 69 °C, starting with the breakdown of the SEI layer, followed by heat production. The temperature window for a mild thermal event and transition to a severe thermal

runaway will then stretch up to above 200 °C, with the onset temperature for TR varying for different cell chemistries. Considering the boiling temperature of the carbonates, it is clear that some can turn to the gas phase early in the heating, while others stay in the liquid phase. This implies that the amount of material in the gas phase and, thus, the internal pressure in the cell can be dependent on the carbonate composition, with a more rapid pressure increase when the carbonates with low boiling temperatures like DMC or EMC (109 °C) are the dominant electrolyte solvent species. The order of boiling points for four common carbonates are as follows: DMC < EMC < DEC < EC. However, the trends for decomposition are different and complicate the situation.

The decomposition of the carbonates is partly dependent on the presence of Li-salt. As shown by Lamb et al. [22], for temperatures up to about 450 °C, the linear carbonates DMC and EMC do not decompose in the studied temperature range if no Li-salt is present. With 1.2 M of LiPF<sub>6</sub>, EMC shows signs of thermal decomposition already at 175 °C, while DMC is not affected. EC and DEC decompose thermally both in the absence and presence of Li-salt, but the decomposition of DEC occurs at a temperature of approximately 100 K lower with salt, while the onset temperature is essentially unchanged for EC. The reactivity of the carbonates in the presence of Li-salt, based on the analysis of the decomposition onset temperature and gas volume, has a trend opposite to that of the boiling point, with EC being the most reactive, followed by DEC, EMC, and DMC.

Yet another factor that needs to be considered for carbonate reactivity is the reaction with O<sub>2</sub>, which takes place at temperatures high enough for oxygen to be released from the cathode. The cyclic EC reacts rather slowly with O<sub>2</sub>, and the thermal decomposition is likely the most important degradation route over a broad temperature range. Among the linear carbonates, DEC tends to be the most reactive towards O<sub>2</sub> since it has longer carbon chains (two ethyl groups) compared to EMC (one ethyl and one methyl group) and the least reactive DMC (two methyl groups).

The difference in hydrocarbon chain length in the carbonates will have implications for the production of small hydrocarbons and, hence, their relative amounts during electrolyte decomposition and reactions.

#### 6.4. Relevance of Measured CO and CO<sub>2</sub> Concentrations

CO and CO<sub>2</sub> are two of the major products in the battery vent gases and can be produced via several different routes during the internal chemical processing in a LIB thermal event. The two compounds originate from hydrocarbon oxidation, and since the main hydrocarbon content in an LIB cell is the carbonates in the electrolyte, one can expect that the amount and composition of carbonates will affect their total amount. However, the availability of chemical reaction partners in the oxidation process, originating from the electrode materials, will affect the relative amounts of CO and CO<sub>2</sub>.

CO<sub>2</sub> is a product of the direct decomposition of the carbonate electrolytes, and as explained in the previous section, carbonates have a different propensity to decompose. CO<sub>2</sub> is also produced when the SEI layer degrades and as a result of reactions of electrode materials. In the presence of O<sub>2</sub> produced inside the cell from the cathode material, carbonates can produce either CO or CO<sub>2</sub> depending on the ratio of O<sub>2</sub> to the carbonate. Lower O<sub>2</sub> concentrations result in incomplete oxidation and more CO production. Another mechanism that can increase CO concentration is when intercalated Li at the anode reduces CO<sub>2</sub> and carbonates to CO.

The processes for CO and CO<sub>2</sub> production, to a large extent, occur simultaneously as the temperature in the LIB cell increases and the chemical composition evolves. It is outside the scope of the present work to investigate the details of the chemical dynamics, but it is relevant to point out that since the reactions have different temperature dependencies, their relative importance changes over time. The degree of chemical pre-processing before the venting starts will affect the ratio, and therefore, there will be differences between, for example, slow thermal abuse that allows significant chemistry to happen inside the LIB

cell before venting starts, and rapid penetration, which is a local event which immediately brings the cell chemicals in contact with external air.

Experimental studies on vent gas composition present scattered results for relative amounts of CO and CO<sub>2</sub>. However, a large number of studies are hampered by limitations in experimental design and gas analysis, and the results are potentially not reliable. The relevant quantity for the assessment of risk for fire and explosion is the composition of the gas as it is vented, while unfortunately, many studies report data representing gas mixtures that have been subject to oxidation external to the battery. Recent reviews include data from different study designs. First, CO/CO<sub>2</sub> from experiments where combustion occurred after gas release are not relevant to compare to fresh vent gases. However, even in cases where there was no combustion, the oxidation of CO to CO<sub>2</sub> likely occurred in the presence of O<sub>2</sub> and other gas-phase oxidisers if the environment was not inert. Hence, only the CO/CO<sub>2</sub> ratio measured in an inert atmosphere can be considered representative of the vent gas composition.

Since the conversion of CO to CO<sub>2</sub> after venting is suspected in many studies, we also chose to plot the sum of the two components in Figures 2, 4 and 6. It is seen that the sums of the components are in better agreement between the studies compared to the ratio of the individual gases.

### 6.5. Dependence on SOC and Cathode Chemistry

There is consensus in the literature that gas compositions from LIBs venting vary depending on cathode chemistry and SOC, but unfortunately, the experimental data are scattered, with studies pointing at different trends. As revealed in the present work, experimental design, gas analysis techniques, and the interpretation of data affect the results. The consequence of this is that different studies are not comparable because they are performed with different prerequisites. In the present work, an effort was made to identify datasets that represent vent gases prior to combustion and without effects from the external environment. Despite this, the data show significant variability, but there are some trends that can be identified.

From the data selected in this study for LFP, NMC, and NCA LIBs, as plotted in Figures 2–7, it can be concluded that over the full range of SOCs, the relative concentration of inert CO<sub>2</sub> decreases and the more reactive components, including CO, increase as SOC increases. There is a weak trend of increasing CO levels at a higher SOC range, above about 75%. Some trends connected to the cathode chemistries are seen, for example, that LFP produce low concentrations of CO. However, the trends should be seen as indications, not as proof, due to the limited data available.

An example which indicates that cathode chemistry is not necessarily the main factor affecting the gas composition is the study on NCA cylindrical LIB cells by Lammer et al. This study shows that although the cells have the same cathode chemistry and an almost identical nominal capacity, the gas compositions are quite different in repetitive tests. The most extreme difference is found in the relative amount of H<sub>2</sub> in the released gases, which ranges from about 18 to 42%. Considering that this difference is seen in the same study with identical experimental methodology, it is one of the most striking examples that cathode chemistry may not be a strong determining factor for gas composition.

## 7. Conclusions and Outlook

In the present work, experimental studies on the composition of vented gases from LIBs were reviewed. As discussed in detail in previous sections, the use of different experimental designs and measurement methods hamper the potential to draw general conclusions from the datasets. In some cases, the usefulness of studies is limited not by the quality of the study but by the lack of detailed explanation of samples or methodologies. The repeatability and reproducibility of test results rely on good experimental planning and the control of all test parameters. Test results in currently available publications on LIB

gassing offer a scattered picture, and their comparison is challenging due to differences in how the experiments were conducted as well as what data were collected and reported.

The datasets from vent gas studies are valuable for the assessment of fire safety and toxicity and can contribute to the development of mitigation strategies. An experimental investigation of LIB venting ideally reports on mass loss and total gas volume and provides complete speciation with the accurate quantification of flammable substances. In addition, to reveal the sources of gases, it is highly beneficial if the tested LIB cells are completely characterised, including the weight of active and passive materials and the composition of the electrolyte. For multi-cell assemblies and battery-level tests, information about battery layout and cell connections, as well as quantified amounts of other flammable materials present in the battery that may contribute to the gaseous emissions, is needed to make the correct assessment of the released gases. The experimental studies on venting presented in Section 5 of the present work are summarised in Table 12 as a guide for the level of information given in the published studies.

**Table 12.** Summary of data collected in different studies. Abbreviations: UH—uniform heating, P—penetration, OC—over-charge. Legend: Trig.—trigger method; Char.—complete characterisation of battery; Mass.—mass loss; TGV—total gas volume; Spec.—complete speciation; Quant.—quantification. (x) in the speciation column means that speciation is extensive but not complete on the main compounds.

	Trig.	Char.	Mass	TGV	Spec.	Quant.	Comments
Zhang et al. (2024) [79]	UH	-	x	x	x	-	Speciation up to C2
Yang et al. (2023) [73]	UH	-	x	x	x	x	-
Willstrand et al. (2023) [14]	UH	-	x	x	x	-	-
Abbott et al. (2023) [84]	UH	-	x	x	x	-	-
Amano et al. (2023) [80]	UH	-	x	x	(x)	x	No H <sub>2</sub> detection
Abbott et al. (2022) [63]	UH	-	-	x	x	x	-
Amano et al. (2022) [81]	UH	-	x	x	(x)	x	No H <sub>2</sub> detection
Cai et al. (2021) [64]	OC	-	-	-	-	-	-
Essl et al. (2021) [9]	UH	x	x	x	x	x	Influence of ageing
Hoelle et al. (2021) [69]	P	-	-	-	-	-	-
Kennedy et al. (2021) [85]	UH	x	x	x	x	x	-
Essl et al. (2020) [61]	UH, P, OC	x	x	x	x	x	-
Essl et al. (2020) [60]	UH	x	x	x	x	x	-
Robles and Jeevarajan (2020) [74]	UH	-	-	x	x	x	Upscaling; electrolyte composition not known
Yuan et al. (2020) [26]	UH	-	-	x	-	x	All gases (carbonates) not detected
Sturk et al. (2019) [75]	UH	-	-	x	x	-	Good speciation; incomplete quantification
Gully (2019) [76]	UH, OC	-	-	x	(x)	x	No H <sub>2</sub> detection
Diaz et al. (2019) [44]	UH, P	-	x	x	x	-	Detection of carbonates and F-compounds; electrolyte composition not known
Fernandes et al. (2018) [4]	OC	x	x	x	x	x	Complete characterisation of LIB
Koch et al. (2018) [68]	UH	-	x	x	x	x	Many cells evaluated together
Koch et al. (2018) [68]	P	-	x	x	-	x	Modules
Lammer et al. (2018) [18]	UH	-	-	x	-	x	Various storage scenarios
Lammer et al. (2017) [35]	UH	-		x	-		-
Gully (2019) [76]	UH			x	x	x	-

**Table 12.** *Cont.*

	Trig.	Char.	Mass	TGV	Spec.	Quant.	Comments
Maloney (2016) [77]	UH	-	-	x	-	x	Performed upscaling experiment; SOC range
Nedjalkov et al. (2016) [70]	P	x	x	x	-	-	
Bergström et al. [78]	UH	-	-	-	x	x	Focus on speciation/toxicology; SOC not given
Yuan et al. (2015) [71]	OC	x	-	-	(x)	-	
Golubkov et al. (2015) [39]	UH	x	x	x	-	x	Characterisation of LIB; electrolyte not detected
Golubkov et al. (2014) [62]	UH	x	x	x	-	x	-
Abraham et al. (2006) [27]	UH	x	-	x	-	x	-
Crafts et al. (2004) [83]	UH	x	-	x	x	x	-

While new and improved experimental studies on LIB cell TRs are essential for increased understanding, it is also important to increase the fundamental understanding of the underlying chemical and physical processes. A substantially increased understanding at the molecular level can be gained from computational studies, and dedicated experiments can be performed on the component level. The outcome from such research then needs to be aggregated into computational models, taking different aspects into account and investigating their interdependence. Groundbreaking work in the modelling of the thermal runaway in LIB cells has recently been published by García et al. [95,96], and for further detail, we refer to these works and the references therein.

The present work, unfortunately, focuses more on the differences between published studies than on similarities since we believe that it is necessary to bring to the common understanding that general conclusions cannot be drawn from the bulk of the studies reporting on the gas composition of vent gases from LIBs. To mitigate this, the present review has highlighted some important factors to consider in future experiments to improve comparability:

1. Detailed information about the test object, e.g., the cell type and size, cell chemistry, and composition of materials, including electrolyte solvent composition;
2. The TR trigger condition to determine the severity of the abuse;
3. Clarity regarding what gases (e.g., vent gases, combustion gases or a mix) are studied;
4. The timing and method of gas measurement (e.g., direct measurement or delayed measurement on sampled gases) as this affects the chemical history of the gases due to the reactivity of some species;
5. Controlled gas environment, e.g., turbulent or stationary conditions, inert or air atmosphere, and gas chamber volume;
6. When evaluating the gas measurements, it is also important to consider the possibility of other oxidants in addition to O<sub>2</sub>, and it is recommended to perform a mass balance to the greatest extent possible in order to verify the consistency of results.

Another aspect that needs to be highlighted is the interpretation of TR trigger methods. TR is triggered in order to simulate internal short circuit conditions and evaluate cell and battery safety performance for this fault condition. However, it is important to remember that all current test methods rely on forced thermal runaway abuse triggers that introduce some level of acceleration compared to spontaneous internal short circuit events, either in the form of added energy or by creating multiple shorting conditions inside the triggered cell.

When choosing the trigger method, it is important to consider its relevance to the real-world condition it aims to simulate. For the analysis of the heat production and the temperature increase and acceleration of chemical reactions, it is important to consider if this is an effect of energy transferred to the system (via the trigger) or originating from the system. The TR trigger method affects the test results since gassing reactions depend on the

dynamics of the chemical reactions, especially the speed of the reaction. Slow TR initiation, such as the homogeneous heating of the entire cell, favours higher relative amounts of CO<sub>2</sub>, whereas fast triggers, like nail penetration or high-power localised heaters, typically lead to incomplete oxidation and higher relative concentrations of CO.

Finally, we would like to stress that the test level influences the TR dynamics, and single-cell results cannot be extrapolated linearly to multi-cell configurations due to the higher temperatures realised in the latter case, which directly impacts the chemical processing and rates of reaction. For highly reactive species, such as HF and POF<sub>3</sub>, the presence of additional surfaces in multi-cell assemblies and batteries reduces the actual gas concentrations due to rapid adsorption and reaction. Vent gas studies on multi-cell configurations are few, and we encourage the research community to take on the challenge of studying these to a larger extent.

**Author Contributions:** Conceptualisation, E.J.K.N. and A.A.T.; methodology, E.J.K.N.; validation, E.J.K.N. and A.A.T.; formal analysis, E.J.K.N. and A.A.T.; investigation, E.J.K.N. and A.A.T.; writing—original draft preparation, E.J.K.N.; writing—review and editing, E.J.K.N. and A.A.T.; visualisation, E.J.K.N.; project administration, E.J.K.N.; funding acquisition, E.J.K.N. and A.A.T. All authors have read and agreed to the published version of the manuscript.

**Funding:** This work was supported by the Swedish Electromobility Centre, funded by the Swedish Energy Agency, with grant number 2019-007869.

**Acknowledgments:** The authors like to acknowledge Intu Sharma and Frej Ryde for their contributions to the early stages of the review process.

**Conflicts of Interest:** Author Annika Ahlberg Tidblad was employed by the company Volvo Car Corporation. The remaining author declares that the research was conducted in the absence of any commercial or financial relationships that could be construed as a potential conflict of interest.

## References

- Wang, X.; Liu, H.; Pan, K.; Huang, R.; Gou, X.Q.; Qiang, Y.J. Exploring thermal hazard of lithium-ion batteries by bibliometric analysis. *J. Energy Storage* **2023**, *67*, 107578. [[CrossRef](#)]
- Wang, Q.S.; Ping, P.; Zhao, X.J.; Chu, G.Q.; Sun, J.H.; Chen, C.H. Thermal runaway caused fire and explosion of lithium ion battery. *J. Power Sources* **2012**, *208*, 210–224. [[CrossRef](#)]
- Wang, Q.S.; Mao, B.B.; Stolarov, S.I.; Sun, J.H. A review of lithium ion battery failure mechanisms and fire prevention strategies. *Prog. Energy Combust. Sci.* **2019**, *73*, 95–131. [[CrossRef](#)]
- Fernandes, Y.; Bry, A.; de Persis, S. Identification and quantification of gases emitted during abuse tests by overcharge of a commercial Li-ion battery. *J. Power Sources* **2018**, *389*, 106–119. [[CrossRef](#)]
- Qiu, M.M.; Liu, J.H.; Cong, B.H.; Cui, Y. Research Progress in Thermal Runaway Vent Gas Characteristics of Li-Ion Battery. *Batteries* **2023**, *9*, 411. [[CrossRef](#)]
- Ghiji, M.; Edmonds, S.; Moinuddin, K. A Review of Experimental and Numerical Studies of Lithium Ion Battery Fires. *Appl. Sci.* **2021**, *11*, 1247. [[CrossRef](#)]
- Rappsilber, T.; Yusfi, N.; Kruger, S.; Hahn, S.K.; Fellinger, T.P.; von Nidda, J.K.; Tschirschwitz, R. Meta-analysis of heat release and smoke gas emission during thermal runaway of lithium-ion batteries. *J. Energy Storage* **2023**, *60*, 106579. [[CrossRef](#)]
- Bugryniec, P.J.; Resendiz, E.G.; Nwophoke, S.M.; Khanna, S.; James, C.; Brown, S.F. Review of gas emissions from lithium-ion battery thermal runaway failure—Considering toxic and flammable compounds. *J. Energy Storage* **2024**, *87*, 111288. [[CrossRef](#)]
- Essl, C.; Golubkov, A.W.; Fuchs, A. Influence of Aging on the Failing Behavior of Automotive Lithium-Ion Batteries. *Batteries* **2021**, *7*, 23. [[CrossRef](#)]
- Broussely, M.; Biensan, P.; Bonhomme, F.; Blanchard, P.; Herreyre, S.; Nechev, K.; Staniewicz, R.J. Main aging mechanisms in Li ion batteries. *J. Power Sources* **2005**, *146*, 90–96. [[CrossRef](#)]
- Thompson, L.M.; Harlow, J.E.; Eldesoky, A.; Bauer, M.K.G.; Cheng, J.H.; Stone, W.S.; Taskovic, T.; McFarlane, C.R.M.; Dahn, J.R. Study of Electrolyte and Electrode Composition Changes vs Time in Aged Li-Ion Cells. *J. Electrochem. Soc.* **2021**, *168*, 020532. [[CrossRef](#)]
- Claassen, M.; Bingham, B.; Chow, J.C.; Watson, J.G.; Chu, P.B.; Wang, Y.; Wang, X.L. Characterization of Lithium-Ion Battery Fire Emissions-Part 2: Particle Size Distributions and Emission Factors. *Batteries* **2024**, *10*, 366. [[CrossRef](#)]
- Claassen, M.; Bingham, B.; Chow, J.C.; Watson, J.G.; Wang, Y.; Wang, X.L. Characterization of Lithium-Ion Battery Fire Emissions-Part 1: Chemical Composition of Fine Particles (PM<sub>2.5</sub>). *Batteries* **2024**, *10*, 301. [[CrossRef](#)]
- Willstrand, O.; Pushp, M.; Andersson, P.; Brandell, D. Impact of different Li-ion cell test conditions on thermal runaway characteristics and gas release measurements. *J. Energy Storage* **2023**, *68*, 107785. [[CrossRef](#)]

15. Raghibi, M.; Xiong, B.K.; Phadke, S.; Anouti, M. Role of the electrolyte in gas formation during the cycling of a Gr//NMC battery as a function of temperature: Solvent, salt, and ionic liquid effect. *Electrochim. Acta* **2020**, *362*, 137214. [[CrossRef](#)]
16. Scharf, J.; von Lüders, C.; Matysik, F.M.; Misiewicz, C.; Wandt, J.; Berg, E.J. Gas evolution in large-format automotive lithium-ion battery during formation: Effect of cell size and temperature. *J. Power Sources* **2024**, *603*, 234419. [[CrossRef](#)]
17. Palacin, M.R. Understanding ageing in Li-ion batteries: A chemical issue. *Chem. Soc. Rev.* **2018**, *47*, 4924–4933. [[CrossRef](#)] [[PubMed](#)]
18. Lammer, M.; Konigseder, A.; Gluschtz, P.; Hacker, V. Influence of aging on the heat and gas emissions from commercial lithium ion cells in case of thermal failure. *J. Electrochem. Sci. Eng.* **2018**, *8*, 101–110. [[CrossRef](#)]
19. Feng, X.N.; Ouyang, M.G.; Liu, X.; Lu, L.G.; Xia, Y.; He, X.M. Thermal runaway mechanism of lithium ion battery for electric vehicles: A review. *Energy Storage Mater.* **2018**, *10*, 246–267. [[CrossRef](#)]
20. Gnanaraj, J.S.; Zinigrad, E.; Asraf, L.; Gottlieb, H.E.; Sprecher, M.; Schmidt, M.; Geissler, W.; Aurbach, D. A detailed investigation of the thermal reactions of LiPF<sub>6</sub> solution in organic carbonates using ARC and DSC. *J. Electrochem. Soc.* **2003**, *150*, A1533–A1537. [[CrossRef](#)]
21. Gnanaraj, J.S.; Zinigrad, E.; Asraf, L.; Gottlieb, H.E.; Sprecher, M.; Aurbach, D.; Schmidt, M. The use of accelerating rate calorimetry (ARC) for the study of the thermal reactions of Li-ion battery electrolyte solutions. *J. Power Sources* **2003**, *119–121*, 794–798. [[CrossRef](#)]
22. Lamb, J.; Orendorff, C.J.; Roth, E.P.; Langendorf, J. Studies on the Thermal Breakdown of Common Li-Ion Battery Electrolyte Components. *J. Electrochem. Soc.* **2015**, *162*, A2131–A2135. [[CrossRef](#)]
23. Maleki, H.; Deng, G.P.; Anani, A.; Howard, J. Thermal stability studies of Li-ion cells and components. *J. Electrochem. Soc.* **1999**, *146*, 3224–3229. [[CrossRef](#)]
24. Roth, E.P.; Doughty, D.H. Thermal abuse performance of high-power 18650 Li-ion cells. *J. Power Sources* **2004**, *128*, 308–318. [[CrossRef](#)]
25. Doughty, D.H.; Roth, E.P.; Crafts, C.C.; Nagasubramanian, G.; Henriksen, G.; Amine, K. Effects of additives on thermal stability of Li ion cells. *J. Power Sources* **2005**, *146*, 116–120. [[CrossRef](#)]
26. Yuan, L.M.; Dubaniewicz, T.; Zlochower, I.; Thomas, R.; Rayyan, N. Experimental study on thermal runaway and vented gases of lithium-ion cells. *Process Saf. Environ. Prot.* **2020**, *144*, 186–192. [[CrossRef](#)]
27. Abraham, D.P.; Roth, E.P.; Kostecki, R.; McCarthy, K.; MacLaren, S.; Doughty, D.H. Diagnostic examination of thermally abused high-power lithium-ion cells. *J. Power Sources* **2006**, *161*, 648–657. [[CrossRef](#)]
28. Fernandes, Y.; Bry, A.; de Persis, S. Thermal degradation analyses of carbonate solvents used in Li-ion batteries. *J. Power Sources* **2019**, *414*, 250–261. [[CrossRef](#)]
29. Eshetu, G.G.; Bertrand, J.P.; Lecocq, A.; Grugeon, S.; Laruelle, S.; Armand, M.; Marlair, G. Fire behavior of carbonates-based electrolytes used in Li-ion rechargeable batteries with a focus on the role of the LiPF<sub>6</sub> and LiFSI salts. *J. Power Sources* **2014**, *269*, 804–811. [[CrossRef](#)]
30. Liu, C.C.; Shen, W.Y.; Liu, X.Z.; Chen, Y.J.; Ding, C.; Huang, Q. Research on thermal runaway process of 18650 cylindrical lithium-ion batteries with different cathodes using cone calorimetry. *J. Energy Storage* **2023**, *64*, 107175. [[CrossRef](#)]
31. Zhong, G.B.; Mao, B.B.; Wang, C.; Jiang, L.; Xu, K.Q.; Sun, J.H.; Wang, Q.S. Thermal runaway and fire behavior investigation of lithium ion batteries using modified cone calorimeter. *J. Therm. Anal. Calorim.* **2019**, *135*, 2879–2889. [[CrossRef](#)]
32. Fu, Y.Y.; Lu, S.; Li, K.Y.; Liu, C.C.; Cheng, X.D.; Zhang, H.P. An experimental study on burning behaviors of 18650 lithium ion batteries using a cone calorimeter. *J. Power Sources* **2015**, *273*, 216–222. [[CrossRef](#)]
33. Huang, Z.H.; Zhao, C.P.; Li, H.; Peng, W.; Zhang, Z.; Wang, Q.S. Experimental study on thermal runaway and its propagation in the large format lithium ion battery module with two electrical connection modes. *Energy* **2020**, *205*, 117906. [[CrossRef](#)]
34. Liu, P.J.; Liu, C.Q.; Yang, K.; Zhang, M.J.; Gao, F.; Mao, B.B.; Li, H.; Duan, Q.L.; Wang, Q.S. Thermal runaway and fire behaviors of lithium iron phosphate battery induced by over heating. *J. Energy Storage* **2020**, *31*, 101714. [[CrossRef](#)]
35. Lammer, M.; Konigseder, A.; Hacker, V. Holistic methodology for characterisation of the thermally induced failure of commercially available 18650 lithium ion cells. *RSC Adv.* **2017**, *7*, 24425–24429. [[CrossRef](#)]
36. Liu, B.H.; Jia, Y.K.; Yuan, C.H.; Wang, L.B.; Gao, X.; Yin, S.; Xu, J. Safety issues and mechanisms of lithium-ion battery cell upon mechanical abusive loading: A review. *Energy Storage Mater.* **2020**, *24*, 85–112. [[CrossRef](#)]
37. Guerrero-Pérez, M.O.; Patience, G.S. Experimental methods in chemical engineering: Fourier transform infrared spectroscopy-FTIR. *Can. J. Chem. Eng.* **2020**, *98*, 25–33. [[CrossRef](#)]
38. Laajimi, H.; Galli, F.; Patience, G.S.; Schieppati, D. Experimental methods in chemical engineering: Gas chromatography-GC. *Can. J. Chem. Eng.* **2022**, *100*, 3123–3144. [[CrossRef](#)]
39. Golubkov, A.W.; Scheikl, S.; Planteu, R.; Voitic, G.; Wiltsche, H.; Stangl, C.; Fauler, G.; Thaler, A.; Hacker, V. Thermal runaway of commercial 18650 Li-ion batteries with LFP and NCA cathodes—Impact of state of charge and overcharge. *RSC Adv.* **2015**, *5*, 57171–57186. [[CrossRef](#)]
40. Golubkov, A.W.; Planteu, R.; Krohn, P.; Rasch, B.; Brunnsteiner, B.; Thaler, A.; Hacker, V. Thermal runaway of large automotive Li-ion batteries. *RSC Adv.* **2018**, *8*, 40172–40186. [[CrossRef](#)]
41. Koch, S.; Fill, A.; Birke, K.P. Comprehensive gas analysis on large scale automotive lithium-ion cells in thermal runaway. *J. Power Sources* **2018**, *398*, 106–112. [[CrossRef](#)]

42. Zhang, Y.; Wang, H.; Li, W.; Li, C. Quantitative identification of emissions from abused prismatic Ni-rich lithium-ion batteries. *eTransportation* **2019**, *2*, 100031. [[CrossRef](#)]
43. Du Pasquier, A.; Disma, F.; Bowmer, T.; Gozdz, A.S.; Amatucci, G.; Tarascon, J.M. Differential scanning calorimetry study of the reactivity of carbon anodes in plastic Li-ion batteries. *J. Electrochem. Soc.* **1998**, *145*, 472–477. [[CrossRef](#)]
44. Diaz, F.; Wang, Y.F.N.; Weyhe, R.; Friedrich, B. Gas generation measurement and evaluation during mechanical processing and thermal treatment of spent Li-ion batteries. *Waste Manag.* **2019**, *84*, 102–111. [[CrossRef](#)] [[PubMed](#)]
45. Ravdel, B.; Abraham, K.M.; Gitzendanner, R.; DiCarlo, J.; Lucht, B.; Campion, C. Thermal stability of lithium-ion battery electrolytes. *J. Power Sources* **2003**, *119*, 805–810. [[CrossRef](#)]
46. Yang, H.; Zhuang, G.V.; Ross, P.N. Thermal stability of LiPF<sub>6</sub> salt and Li-ion battery electrolytes containing LiPF<sub>6</sub>. *J. Power Sources* **2006**, *161*, 573–579. [[CrossRef](#)]
47. Kawamura, T.; Okada, S.; Yamaki, J. Decomposition reaction of LiPF<sub>6</sub>-based electrolytes for lithium ion cells. *J. Power Sources* **2006**, *156*, 547–554. [[CrossRef](#)]
48. Campion, C.L.; Li, W.T.; Lucht, B.L. Thermal decomposition of LiPF<sub>6</sub>-based electrolytes for lithium-ion batteries. *J. Electrochem. Soc.* **2005**, *152*, A2327–A2334. [[CrossRef](#)]
49. Wilken, S.; Treskow, M.; Scheers, J.; Johansson, P.; Jacobsson, P. Initial stages of thermal decomposition of LiPF<sub>6</sub>-based lithium ion battery electrolytes by detailed Raman and NMR spectroscopy. *RSC Adv.* **2013**, *3*, 16359–16364. [[CrossRef](#)]
50. Solchenbach, S.; Metzger, M.; Egawa, M.; Beyer, H.; Gasteiger, H.A. Quantification of PF<sub>5</sub> and POF<sub>3</sub> from Side Reactions of LiPF<sub>6</sub> in Li-Ion Batteries. *J. Electrochem. Soc.* **2018**, *165*, A3022–A3028. [[CrossRef](#)]
51. Botte, G.G.; White, R.E.; Zhang, Z.M. Thermal stability of LiPF<sub>6</sub>-EC: EMC electrolyte for lithium ion batteries. *J. Power Sources* **2001**, *97*–*98*, 570–575. [[CrossRef](#)]
52. Wang, Q.S.; Sun, J.H.; Yao, X.L.; Chen, C.H. C80 calorimeter studies of the thermal behavior of LiPF<sub>6</sub> solutions. *J. Solut. Chem.* **2006**, *35*, 179–189. [[CrossRef](#)]
53. Wilken, S.; Johansson, P.; Jacobsson, P. Infrared spectroscopy of instantaneous decomposition products of LiPF<sub>6</sub>-based lithium battery electrolytes. *Solid State Ion.* **2012**, *225*, 608–610. [[CrossRef](#)]
54. Lekgoathi, M.D.S.; Vilakazi, B.M.; Wagener, J.B.; Le Roux, J.P.; Moolman, D. Decomposition kinetics of anhydrous and moisture exposed LiPF<sub>6</sub> salts by thermogravimetry. *J. Fluor. Chem.* **2013**, *149*, 53–56. [[CrossRef](#)]
55. Okamoto, Y. Ab Initio Calculations of Thermal Decomposition Mechanism of LiPF<sub>6</sub>-Based Electrolytes for Lithium-Ion Batteries. *J. Electrochem. Soc.* **2013**, *160*, A404–A409. [[CrossRef](#)]
56. Yamaki, J.; Shinjo, Y.; Doi, T.; Okada, S.; Ogumi, Z. The Rate Equation of Decomposition for Electrolytes with LiPF<sub>6</sub> in Li-Ion Cells at Elevated Temperatures. *J. Electrochem. Soc.* **2015**, *162*, A520–A530. [[CrossRef](#)]
57. Tebbe, J.L.; Fuerst, T.F.; Musgrave, C.B. Mechanism of hydrofluoric acid formation in ethylene carbonate electrolytes with fluorine salt additives. *J. Power Sources* **2015**, *297*, 427–435. [[CrossRef](#)]
58. Bertilsson, S.; Larsson, F.; Furlani, M.; Albinsson, I.; Mellander, B.E. Lithium-ion battery electrolyte emissions analyzed by coupled thermogravimetric/Fourier-transform infrared spectroscopy. *J. Power Sources* **2017**, *365*, 446–455. [[CrossRef](#)]
59. Liao, Z.H.; Zhang, S.; Zhao, Y.K.; Qiu, Z.J.; Li, K.; Han, D.; Zhang, G.Q.; Habetler, T.G. Experimental evaluation of thermolysis-driven gas emissions from LiPF<sub>6</sub>-carbonate electrolyte used in lithium -ion batteries. *J. Energy Chem.* **2020**, *49*, 124–135. [[CrossRef](#)]
60. Essl, C.; Golubkov, A.W.; Gasser, E.; Nachtnebel, M.; Zankel, A.; Ewert, E.; Fuchs, A. Comprehensive Hazard Analysis of Failing Automotive Lithium-Ion Batteries in Overtemperature Experiments. *Batteries* **2020**, *6*, 30. [[CrossRef](#)]
61. Essl, C.; Golubkov, A.W.; Fuchs, A. Comparing Different Thermal Runaway Triggers for Two Automotive Lithium-Ion Battery Cell Types. *J. Electrochem. Soc.* **2020**, *167*, 130542. [[CrossRef](#)]
62. Golubkov, A.W.; Fuchs, D.; Wagner, J.; Wiltsche, H.; Stangl, C.; Fauler, G.; Voitic, G.; Thaler, A.; Hacker, V. Thermal-runaway experiments on consumer Li-ion batteries with metal-oxide and olivin-type cathodes. *RSC Adv.* **2014**, *4*, 3633–3642. [[CrossRef](#)]
63. Abbott, K.C.; Buston, J.E.H.; Gill, J.; Goddard, S.L.; Howard, D.; Howard, G.; Read, E.; Williams, R.C.E. Comprehensive gas analysis of a 21700 Li(Ni0.8Co0.1Mn0.1O<sub>2</sub>) cell using mass spectrometry. *J. Power Sources* **2022**, *539*, 231585. [[CrossRef](#)]
64. Cai, T.; Valecha, P.; Tran, V.; Engle, B.; Stefanopoulou, A.; Siegel, J. Detection of Li-ion battery failure and venting with Carbon Dioxide sensors. *eTransportation* **2021**, *7*, 100100. [[CrossRef](#)]
65. Lamb, J.; Orendorff, C.J.; Steele, L.A.M.; Spangler, S.W. Failure propagation in multi-cell lithium ion batteries. *J. Power Sources* **2015**, *283*, 517–523. [[CrossRef](#)]
66. Huang, S.; Du, X.N.; Richter, M.; Ford, J.; Cavalheiro, G.M.; Du, Z.J.; White, R.T.; Zhang, G.S. Understanding Li-Ion Cell Internal Short Circuit and Thermal Runaway through Small, Slow and In Situ Sensing Nail Penetration. *J. Electrochem. Soc.* **2020**, *167*, 090526. [[CrossRef](#)]
67. Lamb, J.; Orendorff, C.J. Evaluation of mechanical abuse techniques in lithium ion batteries. *J. Power Sources* **2014**, *247*, 189–196. [[CrossRef](#)]
68. Koch, S.; Birke, K.P.; Kuhn, R. Fast Thermal Runaway Detection for Lithium-Ion Cells in Large Scale Traction Batteries. *Batteries* **2018**, *4*, 16. [[CrossRef](#)]
69. Hoelle, S.; Scharner, S.; Asanin, S.; Hinrichsen, O. Analysis on Thermal Runaway Behavior of Prismatic Lithium-Ion Batteries with Autoclave Calorimetry. *J. Electrochem. Soc.* **2021**, *168*, 120515. [[CrossRef](#)]
70. Nedjalkov, A.; Meyer, J.; Koehring, M.; Doering, A.; Angelmahr, M.; Dahle, S.; Sander, A.; Fischer, A.; Schade, W. Toxic Gas Emissions from Damaged Lithium Ion Batteries—Analysis and Safety Enhancement Solution. *Batteries* **2016**, *2*, 5. [[CrossRef](#)]

71. Yuan, Q.F.; Zhao, F.G.; Wang, W.D.; Zhao, Y.M.; Liang, Z.Y.; Yan, D.L. Overcharge failure investigation of lithium-ion batteries. *Electrochim. Acta* **2015**, *178*, 682–688. [[CrossRef](#)]
72. Global Technical Regulation No. 20 Electric Vehicle Safety (EVS). 2018. Available online: <https://unece.org/fileadmin/DAM/trans/main/wp29/wp29wgs/wp29gen/wp29registry/ECE-TRANS-18a20e.pdf> (accessed on 12 October 2024).
73. Yang, M.; Rong, M.; Pan, J.; Ye, Y.; Yang, A.; Chu, J.; Yuan, H.; Wang, X. Thermal runaway behavior analysis during overheating for commercial LiFePO<sub>4</sub> batteries under various state of charges. *Appl. Therm. Eng.* **2023**, *230*, 120816. [[CrossRef](#)]
74. Robles, D.J.; Jeevarajan, J. Fire and gas characterization studies for lithium-ion cells and batteries. In Proceedings of the 2020 NASA Aerospace Battery Workshop, Huntsville, AL, USA, 17–19 November 2020.
75. Sturk, D.; Rosell, L.; Blomqvist, P.; Tidblad, A.A. Analysis of Li-Ion Battery Gases Vented in an Inert Atmosphere Thermal Test Chamber. *Batteries* **2019**, *5*, 61. [[CrossRef](#)]
76. Gully, B. *Technical Reference for Li-ion Battery Explosion Risk and Fire Suppression*; 2019-1025, Rev. 4; DNV GL AS Maritime: Høvik, Norway, 2019.
77. Maloney, T. *Lithium Battery Thermal Runaway Vent Gas Analysis*; U.S. Department of Transportation: Washington, DC, USA, 2016.
78. Bergström, U.; Gustafsson, Å.; Hägglund, L.; Lejon, C.; Sturk, D.; Tengel, T. *Vent Gases and Aerosol of Automotive Li-ion LFP and NMC Batteries in Humidified Nitrogen under Thermal Load*; FOI-R—4166-SE; Försvarsets Forskningsinstitut FOI: Stockholm, Sweden, 2015.
79. Zhang, J.; Guo, Q.; Liu, S.; Zhou, C.; Huang, Z.; Han, D. Investigation on gas generation and corresponding explosion characteristics of lithium-ion batteries during thermal runaway at different charge states. *J. Energy Storage* **2024**, *80*, 110201. [[CrossRef](#)]
80. Amano, K.O.A.; Hahn, S.-K.; Butt, N.; Vorwerk, P.; Gimadieva, E.; Tschirschitz, R.; Rappsilber, T.; Krause, U. Composition and Explosibility of Gas Emissions from Lithium-Ion Batteries Undergoing Thermal Runaway. *Batteries* **2023**, *9*, 300. [[CrossRef](#)]
81. Amano, K.O.A.; Hahn, S.K.; Tschirschitz, R.; Rappsilber, T.; Krause, U. An Experimental Investigation of Thermal Runaway and Gas Release of NMC Lithium-Ion Pouch Batteries Depending on the State of Charge Level. *Batteries* **2022**, *8*, 41. [[CrossRef](#)]
82. Chen, S.C.; Wang, Z.R.; Wang, J.H.; Tong, X.; Yan, W. Lower explosion limit of the vented gases from Li-ion batteries thermal runaway in high temperature condition. *J. Loss Prev. Process Ind.* **2020**, *63*, 103992. [[CrossRef](#)]
83. Crafts, C.C.; Doughty, D.H.; McBreen, J.; Roth, E.P. *Advanced Technology Development Program for Lithium-Ion Batteries: Thermal Abuse Performance of 18650 Li-ion Cells*; Sandia National Laboratories (SNL): Albuquerque, NM, USA; Livermore, CA, USA, 2004.
84. Abbott, K.C.; Biston, J.E.H.; Gill, J.; Goddard, S.L.; Howard, D.; Howard, G.E.; Read, E.; Williams, R.C.E. Experimental study of three commercially available 18650 lithium ion batteries using multiple abuse methods. *J. Energy Storage* **2023**, *65*, 107293. [[CrossRef](#)]
85. Kennedy, R.W.; Marr, K.C.; Ezekeye, O.A. Gas release rates and properties from Lithium Cobalt Oxide lithium ion battery arrays. *J. Power Sources* **2021**, *487*, 229388. [[CrossRef](#)]
86. Sun, J.; Li, J.; Zhou, T.; Yang, K.; Wei, S.; Tang, N.; Dang, N.; Li, H.; Qiu, X.; Chen, L. Toxicity, a serious concern of thermal runaway from commercial Li-ion battery. *Nano Energy* **2016**, *27*, 313–319. [[CrossRef](#)]
87. Larsson, F.; Andersson, P.; Blomqvist, P.; Mellander, B.E. Toxic fluoride gas emissions from lithium-ion battery fires. *Sci. Rep.* **2017**, *7*, 10018. [[CrossRef](#)] [[PubMed](#)]
88. Willstrand, O.; Pushp, M.; Ingason, H.; Brandell, D. Uncertainties in the use of oxygen consumption calorimetry for heat release measurements in lithium-ion battery fires. *Fire Saf. J.* **2024**, *143*, 104078. [[CrossRef](#)]
89. Li, W.F.; Wang, H.W.; Zhang, Y.J.; Ouyang, M.G. Flammability characteristics of the battery vent gas: A case of NCA and LFP lithium-ion batteries during external heating abuse. *J. Energy Storage* **2019**, *24*, 11. [[CrossRef](#)]
90. Wang, Y.; Song, Z.; Wang, H.; Li, H.; Zhang, Y.; Li, C.; Zhang, X.; Feng, X.; Lu, L.; Ouyang, M. Experimental research on flammability characteristics and ignition conditions of hybrid mixture emissions venting from a large format thermal failure lithium-ion battery. *J. Energy Storage* **2023**, *59*, 106466. [[CrossRef](#)]
91. Alexandrino, K.; Alzueta, M.U.; Curran, H.J. An experimental and modeling study of the ignition of dimethyl carbonate in shock tubes and rapid compression machine. *Combust. Flame* **2018**, *188*, 212–226. [[CrossRef](#)]
92. Henriksen, M.; Vaagsæther, K.; Lundberg, J.; Forseth, S.; Bjerketvedt, D. Laminar burning velocity of gases vented from failed Li-ion batteries. *J. Power Sources* **2021**, *506*, 230141. [[CrossRef](#)]
93. Henriksen, M.; Vaagsæther, K.; Gaathaug, A.V.; Lundberg, J.; Forseth, S.; Bjerketvedt, D. Laminar Burning Velocity of the Dimethyl Carbonate-Air Mixture Formed by the Li-Ion Electrolyte Solvent. *Combust. Explos.* **2020**, *56*, 383–393. [[CrossRef](#)]
94. Wang, Q.; Jiang, L.; Yu, Y.; Sun, J. Progress of enhancing the safety of lithium ion battery from the electrolyte aspect. *Nano Energy* **2019**, *55*, 93–114. [[CrossRef](#)]
95. García, A.; Micó, C.; Marco-Gimeno, J.; Bernal, A. A tabulation method of Li-ion Thermal Runaway mechanisms for the acceleration of high dimensional simulations. *J. Energy Storage* **2024**, *102*, 113982. [[CrossRef](#)]
96. García, A.; Monsalve-Serrano, J.; Gimeno, J.M.; Egea, J.M.H. Experimental measurement and modeling of the internal pressure in cylindrical lithium-ion battery cells under abuse conditions. *J. Energy Storage* **2024**, *103*, 114288. [[CrossRef](#)]